NATIONAL ADVISORY COMMITTEE FOR AERONAUTICS

TECHNICAL NOTE 4029

TURBULENCE MEASUREMENTS IN MULTIPLE INTERFERING AIR JETS

By James C. Laurence and Jean M. Benninghoff

Lewis Flight Propulsion Laboratory
Cleveland, Ohio

Washington
December 1957

NATIONAL ADVISORY COMMITTEE FOR AERONAUTICS

TECHNICAL NOTE 4029

TURBULENCE MEASUREMENTS IN MULTIPLE INTERFERING AIR JETS

By James C. Laurence and Jean M. Benninghoff

SUMMARY

Turbulent and mean-flow characteristics of several noise-suppression multiple-jet nozzles were determined from hot-wire-anemometer measurements for the flow conditions of Mach number 0.3 and Reynolds number of 2.06×10^6 per foot.

The measurements show that turbulent mixing, as indicated by reduced intensity and scale of turbulence, occurs closer to the nozzle in interfering than in noninterfering jets. The turbulence spectra show that the effect of the multiple jets is to redistribute the energy. The more rapid mixing of the interfering jets and shifting of the spectral energy of the interfering jets may explain, in part, the suppression of noise by these nozzles.

INTRODUCTION

In searching for a nozzle configuration that will serve as a noise-suppression device for turbojet engines, experimenters have, in general, tried configurations of corrugations, teeth, ejectors, and so forth, which have been designed to break up the jet flow quickly and increase mixing of the high-energy stream with the surrounding air. References 1 to 4 describe some of these devices. Investigations have been made of the effectiveness of these suppressors in decreasing the noise output of full-scale engines and also of scale-model jets. However, very little of a fundamental nature has been done to survey the jet streams with the purpose of investigating the turbulent structure of the flow (ref. 2).

A major effort has been made to find a theory to relate the noise generated by the jet to the turbulence in the airflow. Lighthill (ref. 5) in a well-known paper has succeeded in this effort. His theory has been verified in many respects with experimental data. In particular, the eighth-power law (the total acoustic power of a jet is proportional to the eighth power of the jet velocity) has been well established. But it is impossible at the present time to compute the noise output of a jet from experimental (hot-wire) measurements of the turbulence by use of his approach.

A different method, which attempts to relate the noise output (sound power) of a jet to the intensity and scale of the turbulent eddies in the airflow, is described in reference 6. A theory based on Lighthill's assumption that the sound field can be replaced by a field of stationary quadrupoles has been used to derive equations that relate the noise output to the turbulence parameters. This method has had only limited success in calculating the noise output of a jet from hot-wire-anemometer measurements in the jet flow. It has been used to explain some of the observed effects in the noise generated by jets.

Other approaches to the problem of noise of aerodynamic origin are described in references 7 and 8.

To provide the data necessary for the theory of reference 6, detailed measurements were made of the intensity, scale, and spectra of turbulence in a subsonic circular air jet (ref. 9). As a continuation of this objective and to obtain data in other jet-nozzle configurations, the same techniques have been applied to some nozzles that are not circular. The nozzles used are models of those which have been tested for possible use as noise suppressors. One class of jet noise-suppression devices is a linear array of slots located quite close together. This type and the sectored type of reference 2 are quite similar in principle. The individual jets pass downstream and mix both with the surrounding atmosphere and with each other.

If the measure of the amount of turbulent mixing is taken to be the reduction in intensity of the turbulence or a reduction in eddy size (scale of turbulence), then one of the following will describe the mixing: First, the turbulent intensity may be less while the eddy size remains constant; second, the eddy size may be reduced while the intensity remains constant; or third, both the scale and the intensity may be less.

Since there is no evidence that any of these changes takes place in multiple interfering jets, the object of these experiments is to determine the effect of the configurations tested on the intensity and scale of the turbulence in the mixing zone common to two or more interfering jets.

It has been observed also that multiple-jet nozzles of the interfering type can alter the spectrum of the noise generated. These alterations usually take the form of reduced or shifted spectral peaks, shifting of sound power from high to low frequency, or vice versa, over-all reduction of the total sound power, or a combination of these changes. It may be expected, therefore, that corresponding changes will be found in the spectral density curves of the turbulence.

The experiments reported herein were a part of the jet noise-research program of the NACA Lewis laboratory.

SYMBOLS

$\mathscr{F}(f)$	spectral density function of $\overline{u^2}$
f	frequency
$\mathscr{R}$	correlation coefficient
r	radial coordinate
t	time
U	mean stream velocity
u	fluctuating component of velocity in x-direction
x,y,z	right-hand coordinate system with x-axis coinciding with jet centerline
β	nondimensional parameter related to cutoff frequencies of spectrum by eq. (B5) of ref. 9
θ	circumferential coordinate
Λ	characteristic eddy size
ω	angular frequency

Subscripts:

c	core
loc	local
t	time
x	longitudinal

Superscripts:

'	root-mean-square
*	characteristic value

INSTRUMENTATION AND TEST FACILITIES

Jet Nozzles and Test Facilities

To implement the model-jet testing program, a series of nozzles was constructed that could be used on an outside test rig (refs. 10 and 11) for noise measurements. For turbulence measurements these nozzles can be bolted to the plenum chamber of the facility described in reference 9. Of these nozzles, a three-sector nozzle (ref. 2) and a rectangular slotted nozzle with four jets were chosen for this work (see fig. 1). The three-sector nozzles were used in this investigation because of the interest raised by reference 2, while the rectangular slotted nozzle was chosen because it was of a class of good noise suppressors (ref. 4). The distance between the jets in the rectangular slotted nozzle could be varied from a maximum separation of about 3 inches to a minimum of about 3/4 inch. In this investigation the spacers used were 1.19 and 2.95 inches.

None of these nozzles proved to be exactly symmetrical with respect to the flow through the various slots and sectors. It was necessary, therefore, to probe in several directions to determine the magnitude of the asymmetry. Surveys were made in the $\bar{y}$- and $\bar{z}$-directions in the rectangular slots (see fig. 2(b)); but in the three-sector nozzle a full 360° survey was made by rotating the probe about the axis of the jet. The aerodynamic axis of the jet was used, since the position of the probe was adjusted until the greatest symmetry in the flow pattern was attained. Within the limits of error of the measurements, the aerodynamic and geometric centers of the nozzle seem to coincide. In the rectangular slotted nozzle, convergent flow channels were included to help distribute the airflow to all four of the jets (see fig. 2(b)).

Other Instrumentation

The other instruments used were those described in reference 9 except for improvements in recording the data for future use. The hot-wire signals, representing the mean-flow level and the root mean square of the fluctuations, were recorded as a function of position in the jet by a double-pen strip chart (XY) recorder. These recordings were useful in obtaining the turbulent and mean-flow velocity profiles.

TEST PROCEDURE

The experimental procedure was divided into two parts: (1) the mean-flow surveys to obtain the velocity profiles in the jet, and (2) the turbulence surveys with the constant-temperature hot-wire anemometers.

Mean-Flow Survey

Total-pressure readings were recorded on a strip chart as a total-pressure probe was traversed throughout the flow field of the jet. A pressure transducer was used to change the pressure signals to a recordable voltage. From these surveys and the hot-wire traces, the velocity profiles and hot-wire calibrations were obtained.

Turbulence Surveys

The strip chart with two pens was used for the hot-wire surveys. These records were used to obtain profiles of the intensity of turbulence as a function of the location of the probe in the jet.

In addition to these profiles of intensity of turbulence, magnetic tape recordings were made of the hot-wire signals at selected points within the mixing regions of the jets. From these recordings autocorrelations and spectra of the signals were determined as described in reference 9.

ANALYSIS OF DATA

Since the primary interest in this report is in the turbulent structure of the jet, the data were analyzed to yield the intensity, the spectral density, the autocorrelation coefficients, and the eddy size of the turbulence.

Intensity of Turbulence

Some of the turbulence encountered in jets of the kind used in this investigation is very intense. The fluctuating velocities are a large percent of the mean flow. This fact makes the experimental measurement of the velocity fluctuations difficult. The constant-temperature anemometers help somewhat in this difficulty; but, in general, the results are considered to be accurate within 10 percent if the intensities are less than 30 to 40 percent. This problem has been investigated and is discussed in reference 9. (Ref. 12 gives a method for correcting the measurements, but it was not used in this report.)

The hot-wire signals were analyzed to give the intensity of turbulence by the method of reference 13. After the profiles of intensity of turbulence were drawn at selected distances downstream of the jet, contour maps were made showing lines of constant turbulence intensity for various cross sections of the jets.

Scale of Turbulence

The scale of turbulence was obtained from the autocorrelation coefficients $\mathscr{R}_t$ as explained in reference 9. A typical autocorrelogram is well represented by the following empirical expression:

$$\mathscr{R}_t = \frac{e^{-\omega^* t} - \beta e^{-\beta\omega^* t}}{1 - \beta} \tag{1}$$

where β and the angular frequency ω^* are constants that can be evaluated from the experimental correlograms, and t is time. The characteristic frequency ω^*, which is related to the upper and lower cutoff frequencies of the spectrum of turbulence, can be converted to an average eddy size by the equation

$$\Lambda_x = \frac{U_{loc}}{\omega^*} \tag{2}$$

where Λ_x is the eddy size and U_{loc} the local mean velocity.

This method of analysis fails, of course, when the empirical equation does not fit the experimental autocorrelograms. This is particularly true at points in the jet close to the nozzle, where no satisfactory method has been found to evaluate the eddy size. In fact, it may be erroneous to speak of an eddy size here, since eddies in the turbulence sense exist in combination with periodic flow disturbances.

Spectrum of Turbulence

The spectrum provides another approach to the energy distribution of the turbulent velocities. In particular, the spectra show bands of frequencies where the energy content is high and periodicities are present in the velocity fluctuations. These spectra are useful in comparison with those of the circular jet to show how the energy is altered by the nozzle configuration under study. It is possible to spot shifts of energy from one part of the spectrum to another as well as reduction of energy content in certain bands of frequencies.

It is more convenient to measure both the autocorrelations and the spectra of the turbulence rather than to obtain one from the other by means of a Fourier transform. However, reference 9 shows that the two methods give identical results if required.

RESULTS AND DISCUSSION

Mean Flow

Mean-flow maps, three-sector nozzle. - The results of the mean-flow studies are presented in figures 3 and 4. Figure 3 shows the contours of constant velocity to an accuracy of ±10 percent in the 295° to 115° plane through the three-sector nozzle. This plane contains a low-flow region as well as one of the high-speed jets. The contours show an asymmetry probably caused by structural irregularities in the nozzles themselves as well as misalinement of the probes used to measure the velocity of the airstream. The difference in size of the sectors, the roughness of the welds, and the unequal buildup of the boundary layers caused different mass flows of air through the three sectors. This is best shown in figure 4, where a comparison of the constant-velocity lines shows the skewness of the flow. In this nozzle the mass-flow differences are slight.

Figures 4(a) to (e) show cross sections at right angles to the direction of the flow at distances of 2, 4, 8, 16, and 24 inches downstream of the three-sector nozzle. These figures give evidence of some twisting of the flow as it proceeds downstream of the nozzle. A growing core of constant-velocity air around the projected or aerodynamic axis of the nozzle is shown by the disappearance of the $U_{l_{oc}}/U_c$ profiles of 20, 30, and 40 percent as the distance from the nozzle increases. This core contains completely mixed air of constant mean velocity and, as will be seen later, constant turbulence intensity. The size of this core increases as the distance from the nozzle increases.

Mean-flow maps, rectangular slotted nozzle. - Figures 5 and 6 show the mean-flow maps for the rectangular slotted nozzles. Figures 5(a) and (b) show the cross sections in the x-z plane, and figures 6(a) and (b) in the x-y plane. Figure 5(a) shows the flow maps for nozzles spaced 2.95 inches apart, and figure 5(b) for nozzles spaced 1.19 inches apart. These two figures show an asymmetry of flow that can be attributed to unequal boundary-layer buildup within the divergent section, to the convergent flow channels (which directed the air from this section into the nozzles), or to an ejector action after the flow left the nozzles. The asymmetry in the x-y plane is not as prominent as in the x-z plane, but it is clearly evident that there was a larger mass flow of air through the inner nozzles as compared with the outer ones.

A comparison of figures 5(a) and (b) with figures 6(a) and (b) in the x-y and also in the x-z planes shows that the mixing of the high-speed streams with each other and with the entrained air takes place at a faster rate for the narrower spacing. However, the maps in the x-y plane are very similar and are little affected by the nozzle spacing.

In general, these figures show that the differences in the flow maps of the nozzles are small because of structural irregularities but larger because of differences in nozzle spacing.

Turbulent Flow

Intensity of turbulence, three-sector nozzle. - The intensity of turbulence throughout the flow field of the three-sector nozzle has been mapped similarly to the mean flow. The results of the complete survey were averaged and are presented for only one 130° sector of the complete rotation angle, for the following reasons: (1) the mean-flow survey showed only slight differences in the three sectors, and (2) the hot-wire traces show fluctuations of the velocity that are larger than the variations due to asymmetry. Thus, the averaged value presents a true picture of the turbulence level.

Figure 7 shows contours of equal turbulence intensity for planes perpendicular to the direction of flow (r-θ planes) at distances downstream of the nozzle of 2, 4, 8, 12, 16, 20, 24, and 28 inches. Figure 7(a) shows a more or less uniform pattern that starts to break up as the jets begin to mix with the entrained air; the mixing proceeds as shown in the successive figures 7(b) to (h). In 7(a) and (b) the high intensity of turbulence along the regions of greatest shear (the zones where the mixing of the high-speed jet with the room air is taking place) is shown by the closeness of the profiles at the boundaries of the high-speed flow. In 7(c) to (h), where the high-speed cores have disappeared and complete mixing has taken place, the curves show a decay of the jet structure, mixing at the outer extremes with the room air, and the presence of a central core of constant-intensity completely mixed air in which the turbulence has begun to decay.

Intensity of turbulence, rectangular slotted nozzle. - The intensity of turbulence for the rectangular slotted nozzles is mapped in figure 8 for nozzle spacing of 1.19 inches. In these figures are plotted constant turbulence-intensity lines showing the variation of the intensity with distance from the jet nozzles. The map in the x-y plane is given for the first of the rectangular nozzles in figure 8(a), while the maps in the x-z plane are given in figures 8(b) and (c) for the positions outside the first nozzle and between the first and second nozzles.

From these figures it is possible to obtain information on the turbulent mixing of the first jet with the room air alone and the first and second jets with each other as well as with the room air. For instance, figure 8(b) shows that the 8-, 10-, and 12-percent profiles extend farther downstream than they do in figure 8(c), which shows the common mixing zone between the first two jets. The evidence given here shows that the effect of the adjacent jets is to increase the mixing of the jets with

each other and with entrained air from the room. This mixing results in a smaller intensity of turbulence in the common zone between two jets than that found where there is no adjacent jet with which to mix.

Similar experiments were performed with a spacing between nozzles of 2.95 inches. The results, which are similar to those shown for a spacing of 1.19 inches, are not given specifically in this report. Not enough data were taken to determine the effect of the spacing of the nozzles on the jet mixing. Reference 4, however, discusses the effect of the spacing on the sound power output of the nozzles.

Spectrum of turbulence, three-sector nozzle. - Turbulent velocity spectra are usually presented in terms of the spectral density function. This function is the ratio of the kinetic energy per unit band pass to the total kinetic energy over the complete range of frequencies. A spectrum gives useful as well as interesting information about the energy distribution of the flow through the nozzle. Figures 9 and 10 show the spectral density function plotted against the frequency 4 and 8 inches downstream of the nozzle. The set of curves shows the spectra as the axial and radial distances are changed for three different circumferential positions in the three-sector nozzles.

The interesting features are as follows:

(1) The definite peaks in the spectra show the frequency ranges where the predominant energy is located.

(2) A central core of turbulent air grows in the radial direction as the axial distance from the jet nozzle increases. The spectrum of this completely mixed and turbulent air shows no peaks, and the intensity is constant throughout this core.

(3) As the distance from the jet nozzle is increased, the spectra for different circumferential positions become more nearly alike. This fact shows that the turbulent structure has become uniform throughout and the pattern of the lobes is tending to disappear.

Figures 9(a), (b), and (c) give evidence of the spectral peaks mentioned in item (1). In 9(a) the curves indicate a peak at about 100 to 200 cps for all circumferential positions in the jet at a radial distance of 1/2 inch. This indicates the central core described in item (2). As the radial distance increases to $1\frac{1}{2}$ inches (fig. 9(b)), the picture is the same for the circumferential position of 66.7° (the inflow air) with the peak still in the neighborhood of 100 to 200 cps. However, there are still trends toward spectral peaks at 100 to 200 cps in the two positions within the high-speed flow, and an additional spectral peak occurs at 800 to 1000 cps. Figure 9(c) illustrates a similar pattern of flow for a radial distance of $2\frac{1}{2}$ inches. For the two circumferential positions within the

inflow region, the spectral peak has shifted somewhat to about 100 cps, while the spectral peak within the high-flow sector ($\theta = 0^{\circ}$) occurs at 600 to 800 cps.

Figures 9(b) and (c) illustrate also the redistribution of spectral energy by the nozzle configuration. In these figures the rate of decrease in the high-frequency range (about 1000 cps) is much steeper at some positions within the jets than at others. This change in the spectrum indicates a change in the energy content of the flow.

Figure 10, for positions 8 inches downstream of the nozzle, gives spectral peaks similar but less pronounced than those at 4 inches from the nozzle (fig. 9). In 10(a) the curves are very similar and are characteristic of the inner core of turbulent (completely mixed) air. Figures 10(b) and (c) show the development of the secondary peak at 400 to 600 cps until the radial distance is large (figs. 10(d) and (e)), at which positions no discrete peaks exist at 800 to 1000 cps.

Spectrum of turbulence, rectangular slotted nozzle. - For the rectangular slotted nozzle, the spectra in the mixing zone between two nozzles are given in figure 11. Here are displayed the spectra for axial distances from 1 to 20 inches downstream of the nozzle for points in the mixing region halfway between the first and second nozzles. The figures show the effect of mixing of the jets on the spectral density curves. At first (fig. 11(a)) little mixing has occurred and the spectrum shows fluctuations, spectral peaks, and plateaus near 100 and 1000 cps. As the distance from the jets increases, these two peaks merge into one at about 100 to 200 cps.

A sequence similar to that of figure 11 is given in figure 12 for the mixing zone just outside the first nozzle. The figures give the spectra at the same distances from the nozzle as in figure 11. There is less evidence of the spectral peaks that were found in the common mixing region between the two jets.

Scale or Eddy Size

The Λ scale of the turbulence or eddy size was evaluated as described in the ANALYSIS OF DATA section of this report with the results shown in figure 13.

Three-sector nozzle. - In figure 13(a) the variation of the eddy size with distance from the jet nozzle is shown for three positions within the mixing zones of the jets. All the measurements shown are for a radial distance of $1\frac{1}{2}$ inches from the jet centerline of the three-sector nozzle and for three positions: one within one of the three high-speed jets and two within the low-speed zones or mixing air. The variation of the scale

with distance from the nozzle is linear, as it is in a circular nozzle (ref. 9). The scale within the high-speed jet is much smaller than it is in the mixing zones.

Rectangular slotted nozzle. - In figure 13(b) the eddy size is shown as a function of distance from the rectangular slotted nozzle for two selected positions: one in the mixing zone of the first jet alone in the x-z plane and two in the common mixing zone between the first and second jets. The scale in the mixing zone between the first and second jets is larger than that in the mixing zone of the first jet alone from the nozzle exit to about 7 inches downstream. From that point on, the eddy size in the common mixing zone of the first and second jets was very much less than that of the first jet alone.

In this nozzle also, the variation of scale with distance is linear for at least as far as 20 inches downstream.

No nondimensionalizing parameter is known with which comparisons of scale of large and small nozzles and special configurations of nozzles can be made. Hence, results with these two nozzles are not compared quantitatively with a circular nozzle.

CONCLUSIONS

Hot-wire-anemometer measurements of the intensity, scale, and spectra of turbulence in the mixing zones of a three-sector nozzle and a four-jet rectangular slotted nozzle gave the following results:

1. The turbulent mixing (the reduction of turbulent intensity and scale in regions of interference as compared with regions of noninterference) that occurs when a jet exhausts into stationary air is aided by dividing the flow into multiple interfering jets.

2. The scale and intensity of turbulence are less in the common mixing zone of two interfering rectangular jets than in the mixing zone of a single jet of the configuration.

3. The turbulent spectra show that, when a comparison is made of those in the high-speed flow region with those of the low-speed flow, the effect of multiple slots or sectors is to shift energy from high to low frequencies and to eliminate or reduce spectral peaks in certain frequencies and to augment them in others.

Lewis Flight Propulsion Laboratory
National Advisory Committee for Aeronautics
Cleveland, Ohio, May 16, 1957

REFERENCES

1. Westley, R., and Lilley, G. M.: An Investigation of the Noise Field from a Small Jet and Methods for Its Reduction. Rep. No. 53, The College of Aero. (Cranfield), Jan. 1952.

2. Greatrex, F. B.: Jet Noise. Preprint No. 559, Inst. Aero. Sci., June 1955.

3. Withington, Holden W.: Silencing the Jet Aircraft. Aero. Eng. Rev., vol. 15, no. 4, Apr. 1956, pp. 56-63; con't., p. 84.

4. Coles, Willard D., and Callaghan, Edmund E.: Full-Scale Investigation of Several Jet-Engine Noise-Reduction Nozzles. NACA TN 3974, 1957.

5. Lighthill, M. J.: On Sound Generated Aerodynamically. I - General Theory. Proc. Roy. Soc. (London), ser. A, vol. 211, no. 1107, Mar. 20, 1952, pp. 564-587.

6. Sanders, Newell D., and Laurence, James C.: Fundamental Investigation of Noise Generation by Turbulent Jets. Preprint No. 744, SAE, 1956.

7. Proudman, I.: Generation of Noise by Isotropic Turbulence. Proc. Roy. Soc. (London), ser. A, vol. 214, 1952, pp. 119-132.

8. Mawardi, O. K., and Dyer, I.: On Noise of Aerodynamic Origin. Jour. Acoustic Soc. Am., vol. 25, no. 3, May 1953, pp. 389-394.

9. Laurence, James C.: Intensity, Scale, and Spectra of Turbulence in Mixing Region of Free Subsonic Jet. NACA Rep. 1292, 1956. (Supersedes NACA TN's 3561 and 3576.)

10. Callaghan, Edmund E., and Coles, Willard D.: Investigation of Far Noise Field of Jets. I - Effect of Nozzle Shape. NACA TN 3590, 1956.

11. Coles, Willard D., and Callaghan, Edmund E.: Investigation of Far Noise Field of Jets. II - Comparison of Air Jets and Jet Engines. NACA TN 3591, 1956.

12. Schubauer, G. B., and Klebanoff, P. S.: Theory and Application of Hot-Wire Instruments in the Investigation of Turbulent Boundary Layers. NACA WR W-86, 1946. (Supersedes NACA ACR 5K27.)

13. Laurence, James C., and Landes, L. Gene: Auxiliary Equipment and Techniques for Adapting the Constant-Temperature Hot-Wire Anemometer to Specific Problems in Air-Flow Measurements. NACA TN 2843, 1952.

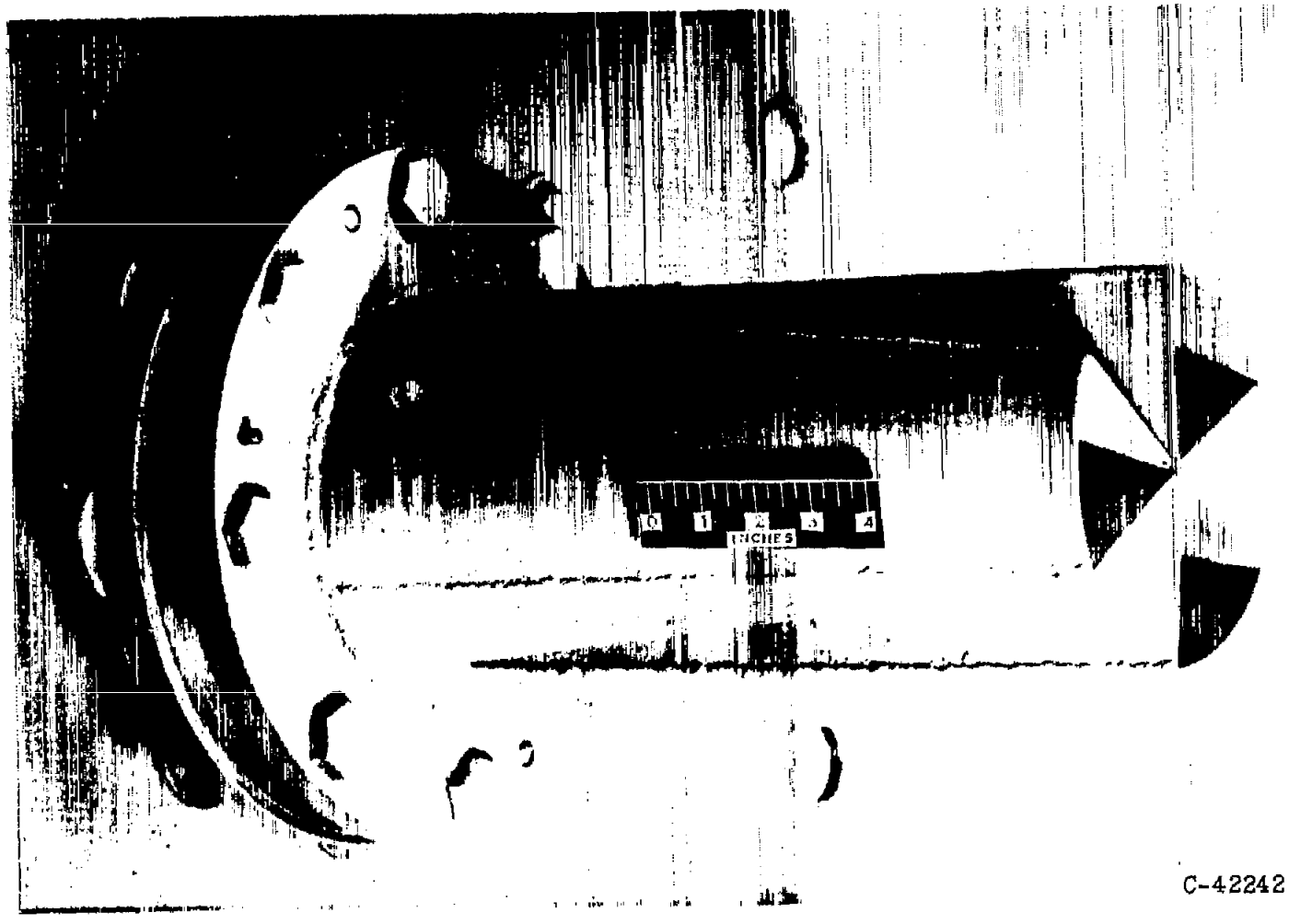

(a) Three-sector nozzle.

Figure 1. - Noise-suppression nozzles.

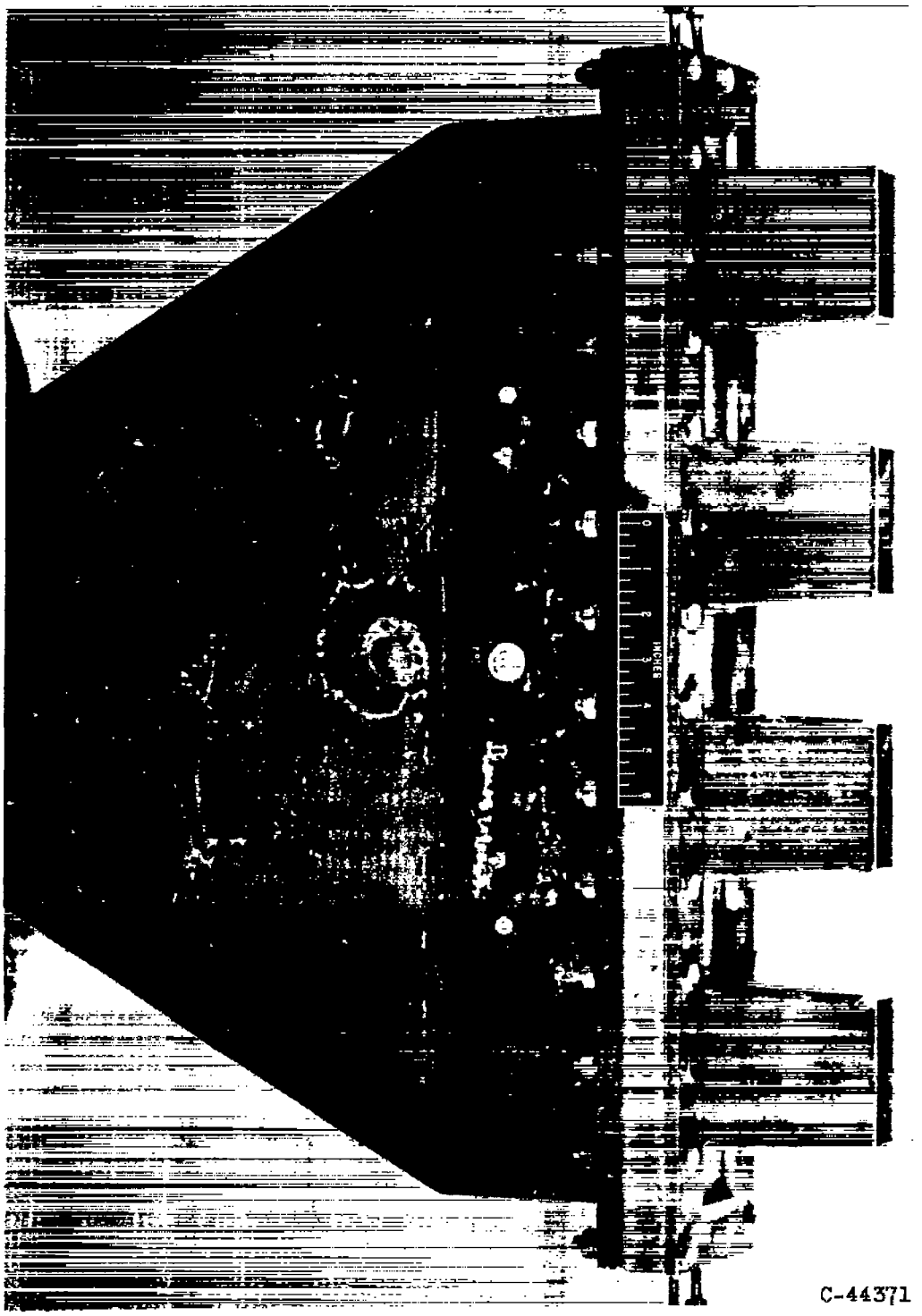

(b) Rectangular slotted nozzle.

Figure 1. - Concluded. Noise-suppression nozzles.

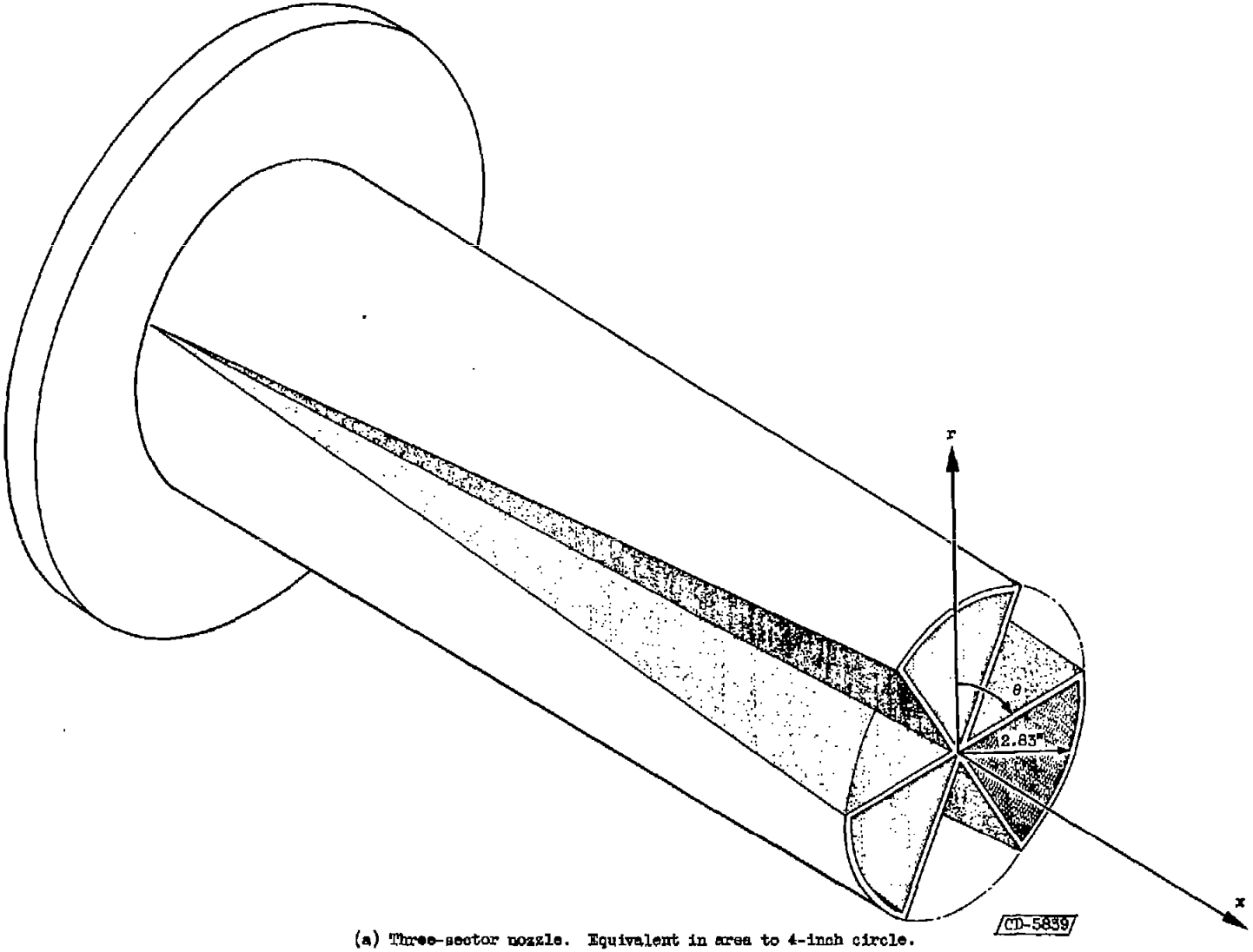

(a) Three-sector nozzle. Equivalent in area to 4-inch circle.

Figure 2. - Coordinate systems of nozzles.

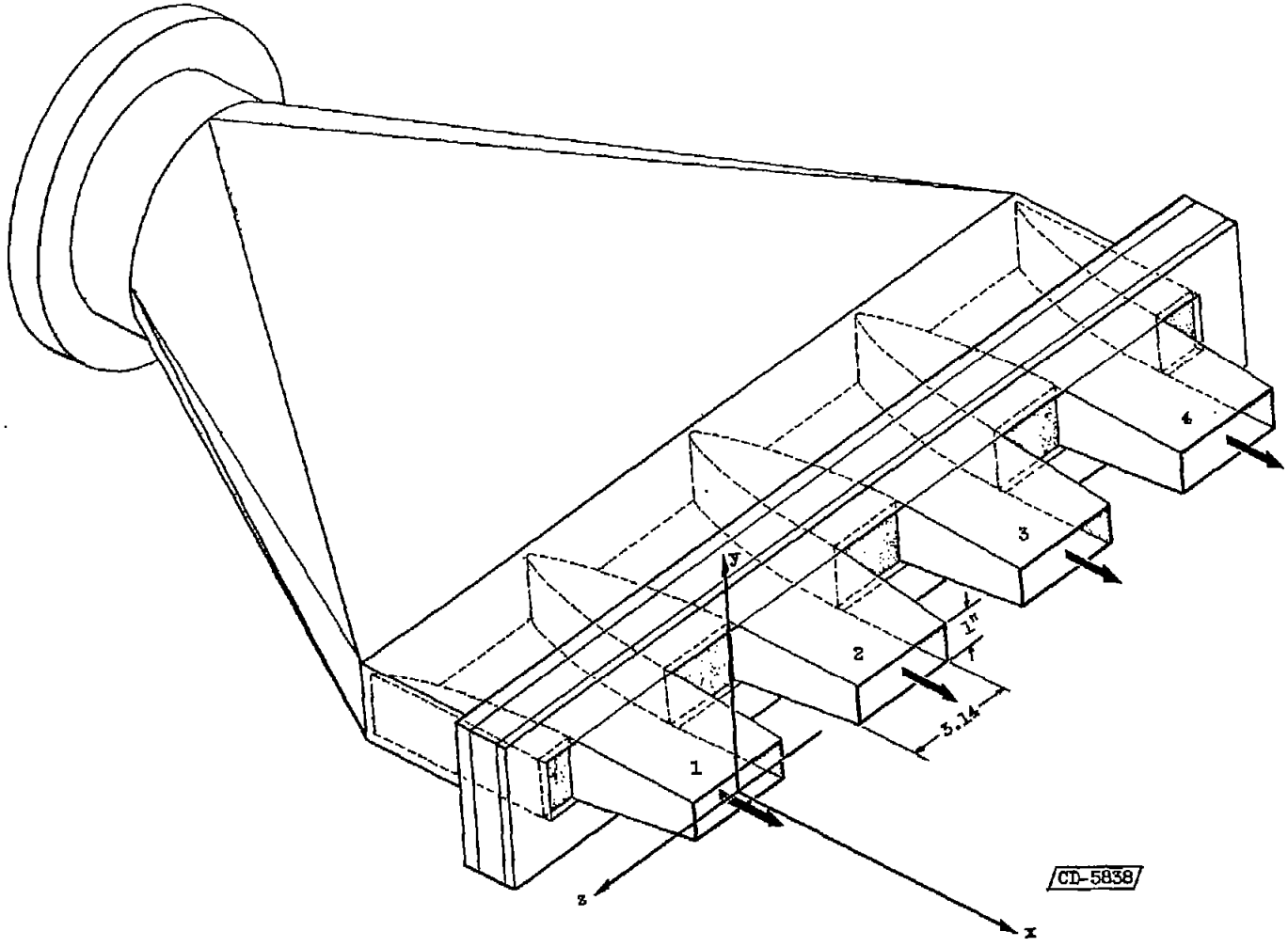

(b) Rectangular slotted nozzles. Equivalent in area to 4-inch circle.

Figure 2. - Concluded. Coordinate systems of nozzles.

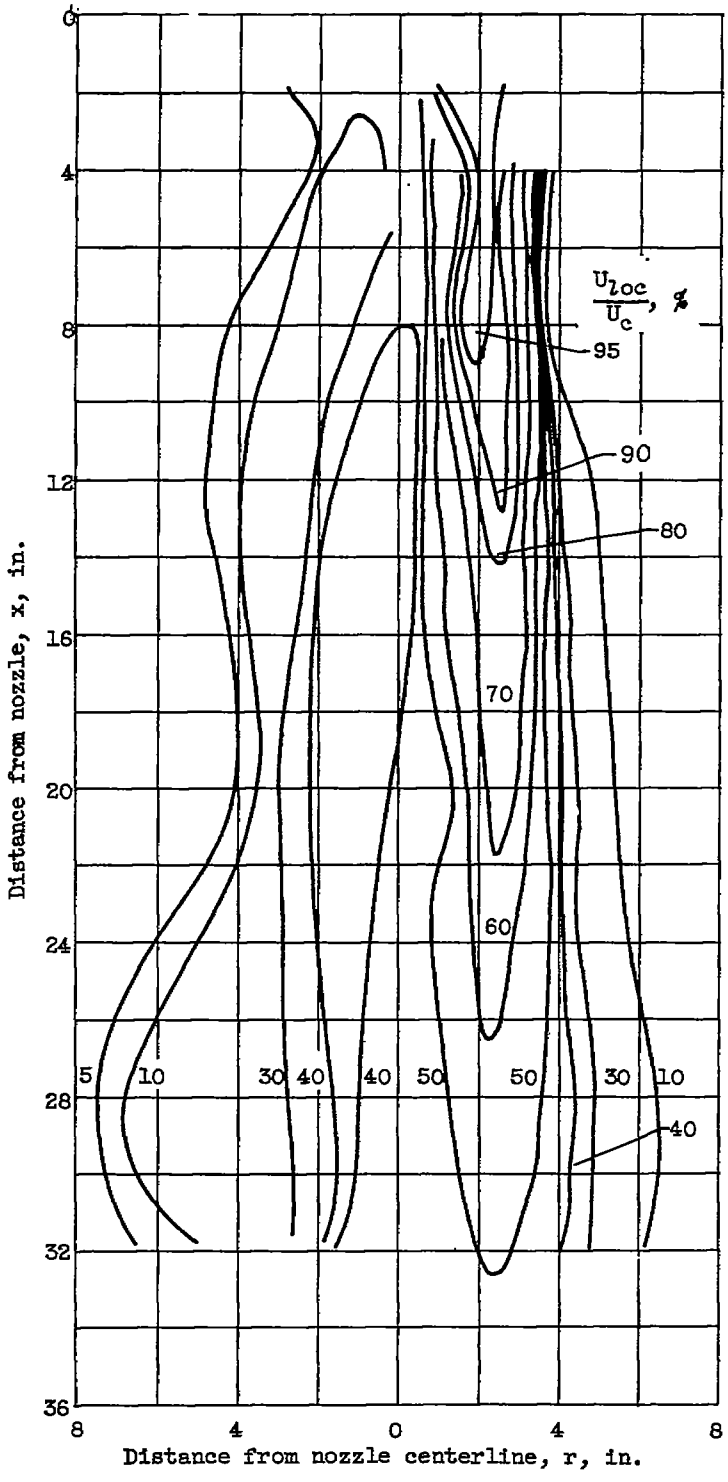

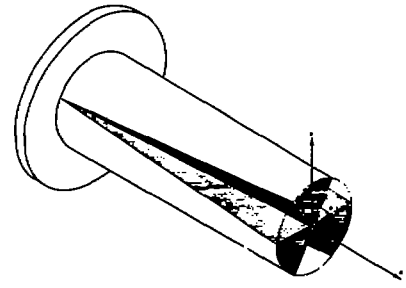

Figure 3. - Mean-flow map for three-sector nozzle at 295° to 115° in r-x plane. Mach number, 0.3; Reynolds number, 2.06×10^6 per foot.

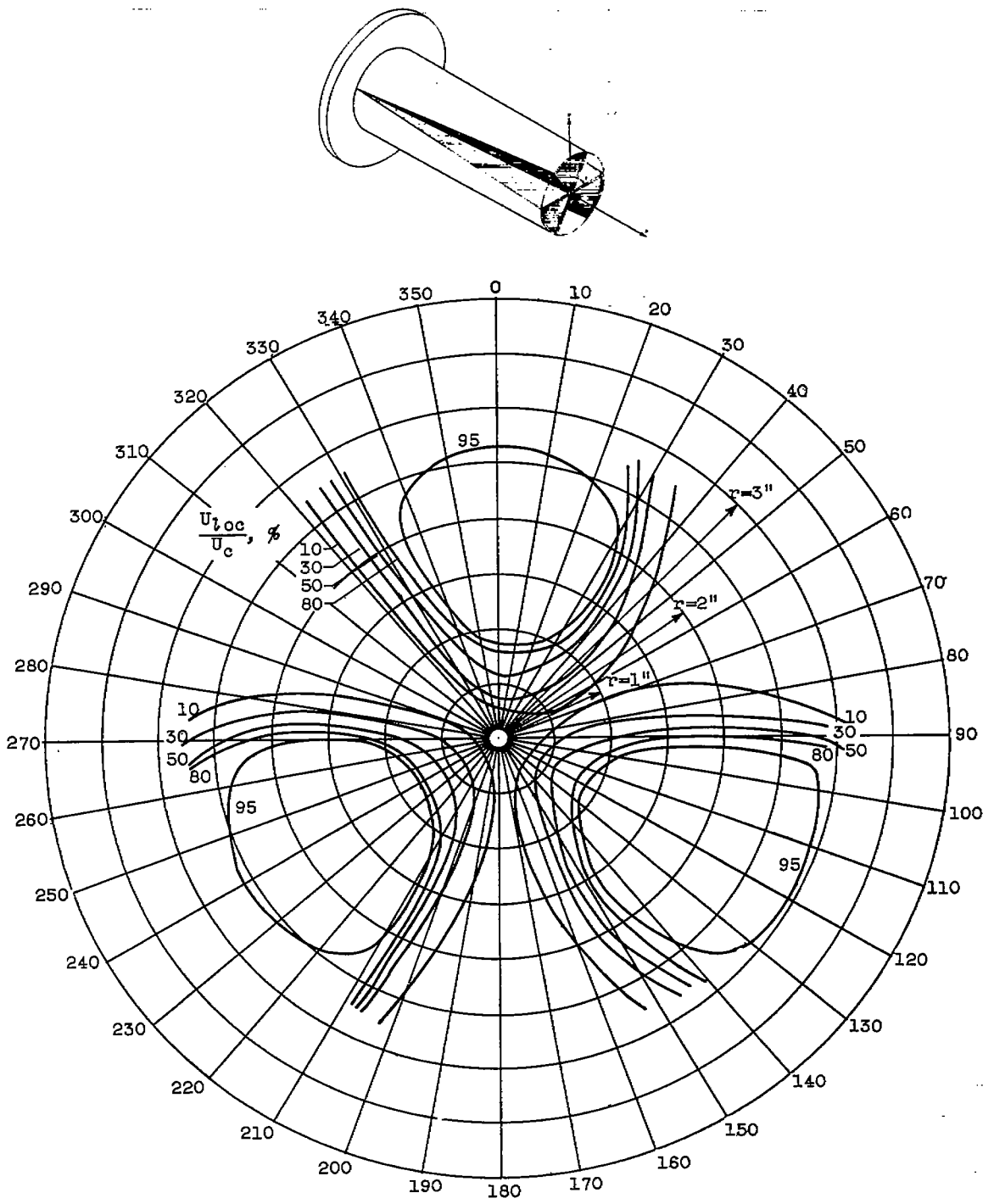

(a) Distance from nozzle, 2 inches.

Figure 4. - Mean-flow maps for three-sector nozzle in x-θ plane. Mach number, 0.3; Reynolds number, 2.06×10^6 per foot.

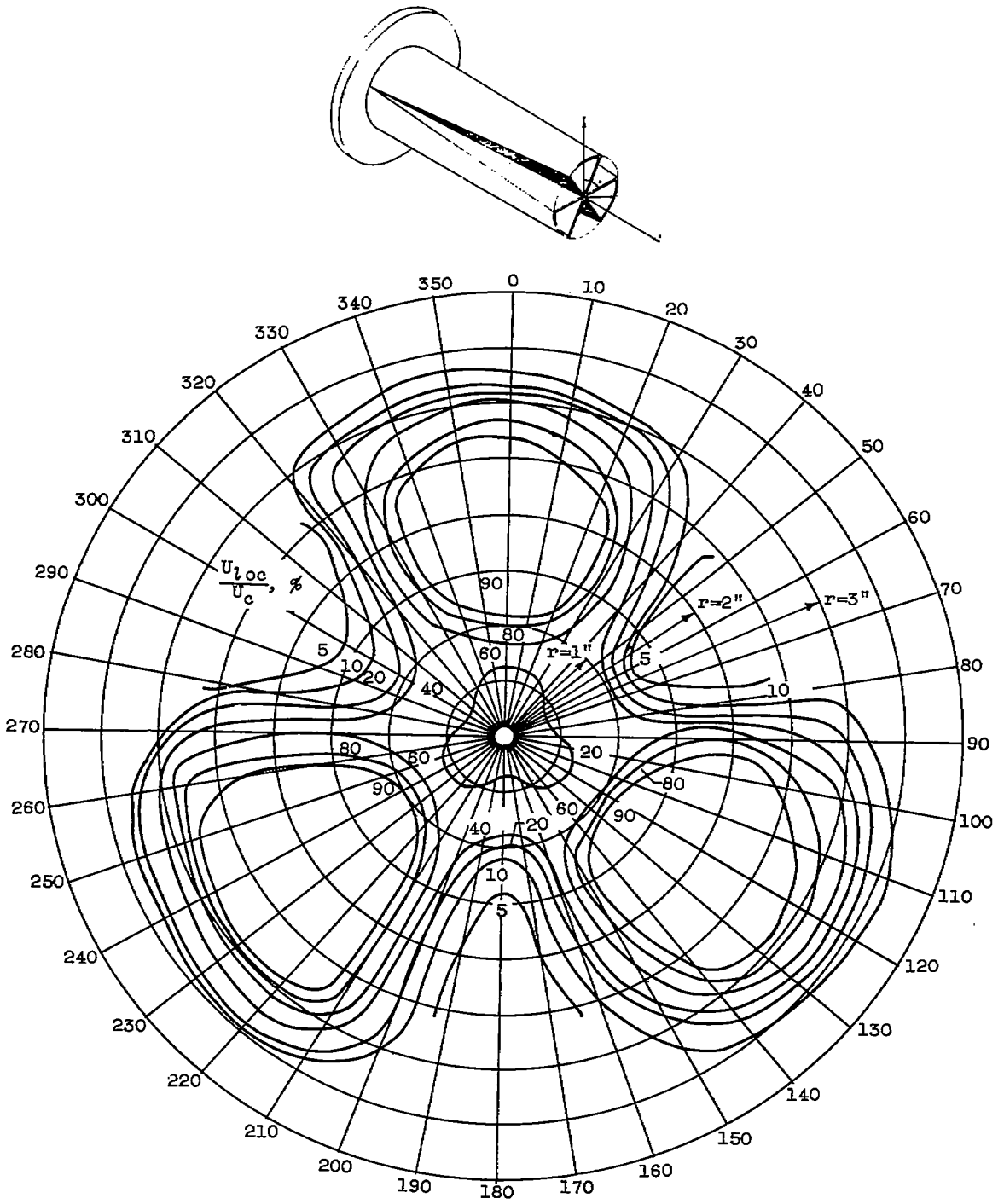

(b) Distance from nozzle, 4 inches.

Figure 4. - Continued. Mean-flow maps for three-sector nozzle in x-θ plane. Mach number, 0.3; Reynolds number, 2.06×10^6 per foot.

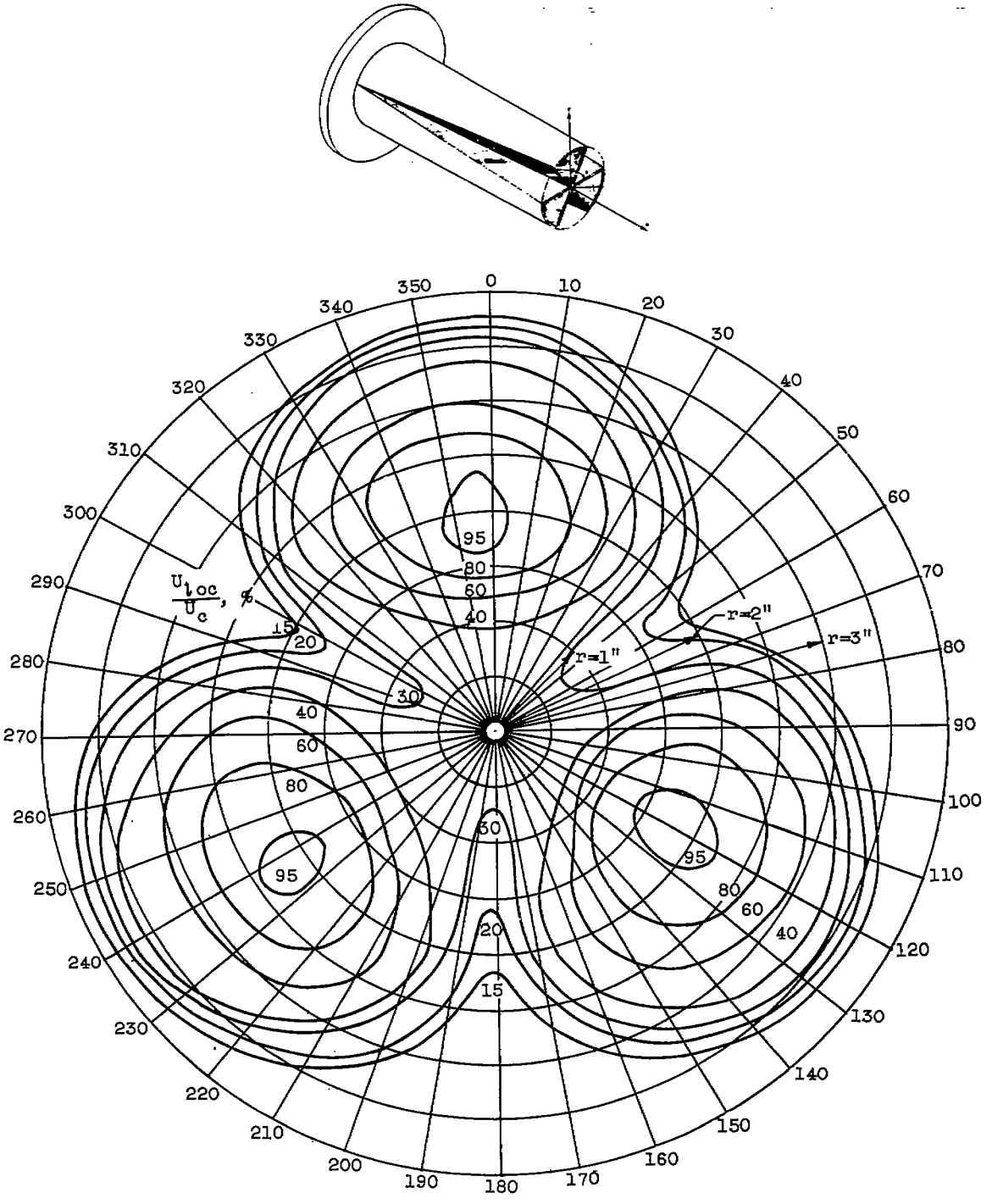

(c) Distance from nozzle, 8 inches.

Figure 4. - Continued. Mean-flow maps for three-sector nozzle in x-θ plane. Mach number, 0.3; Reynolds number, 2.06×10^6 per foot.

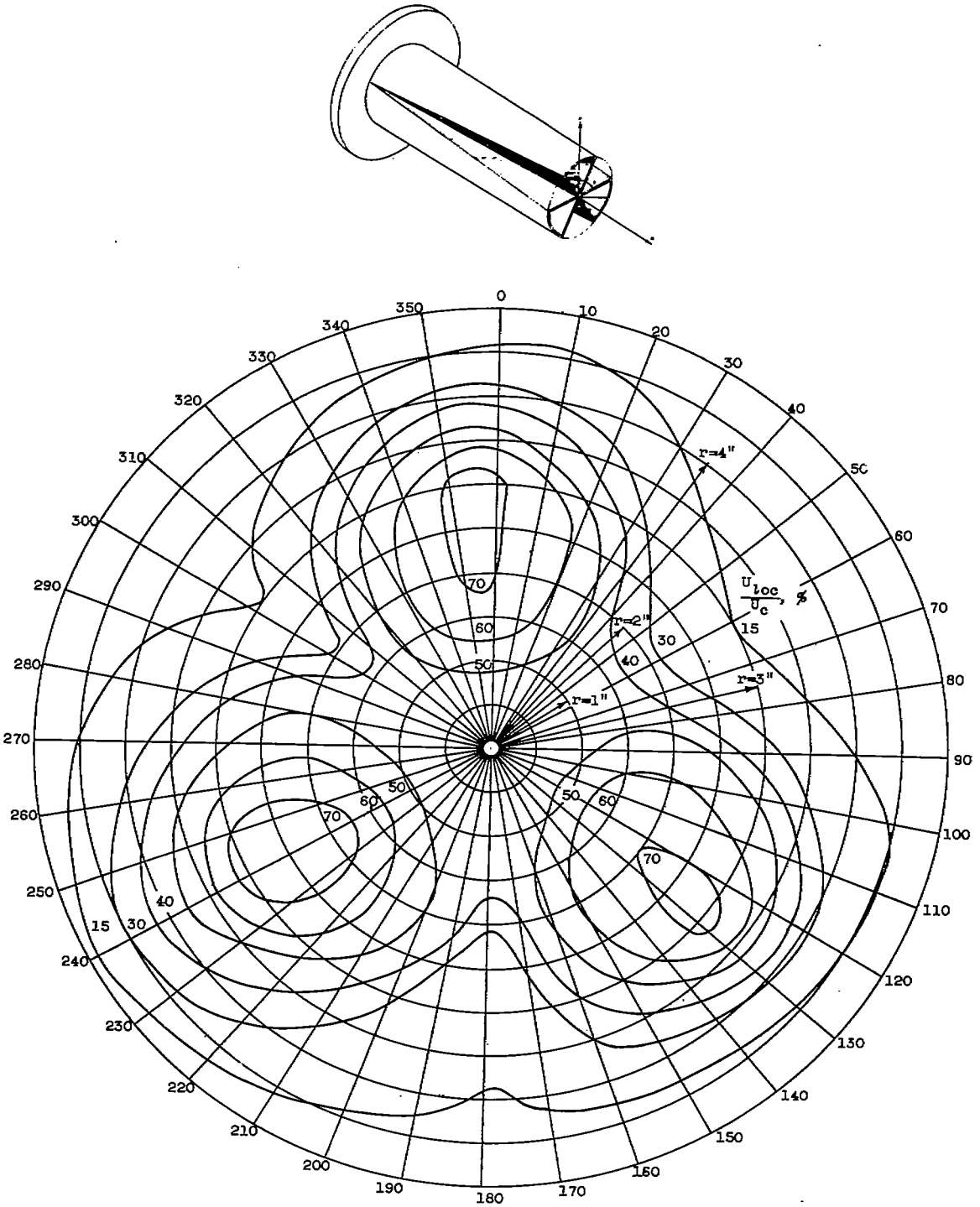

(d) Distance from nozzle, 16 inches.

Figure 4. - Continued. Mean-flow maps for three-sector nozzle in x-θ plane. Mach number, 0.5; Reynolds number, 2.06x10⁶ per foot.

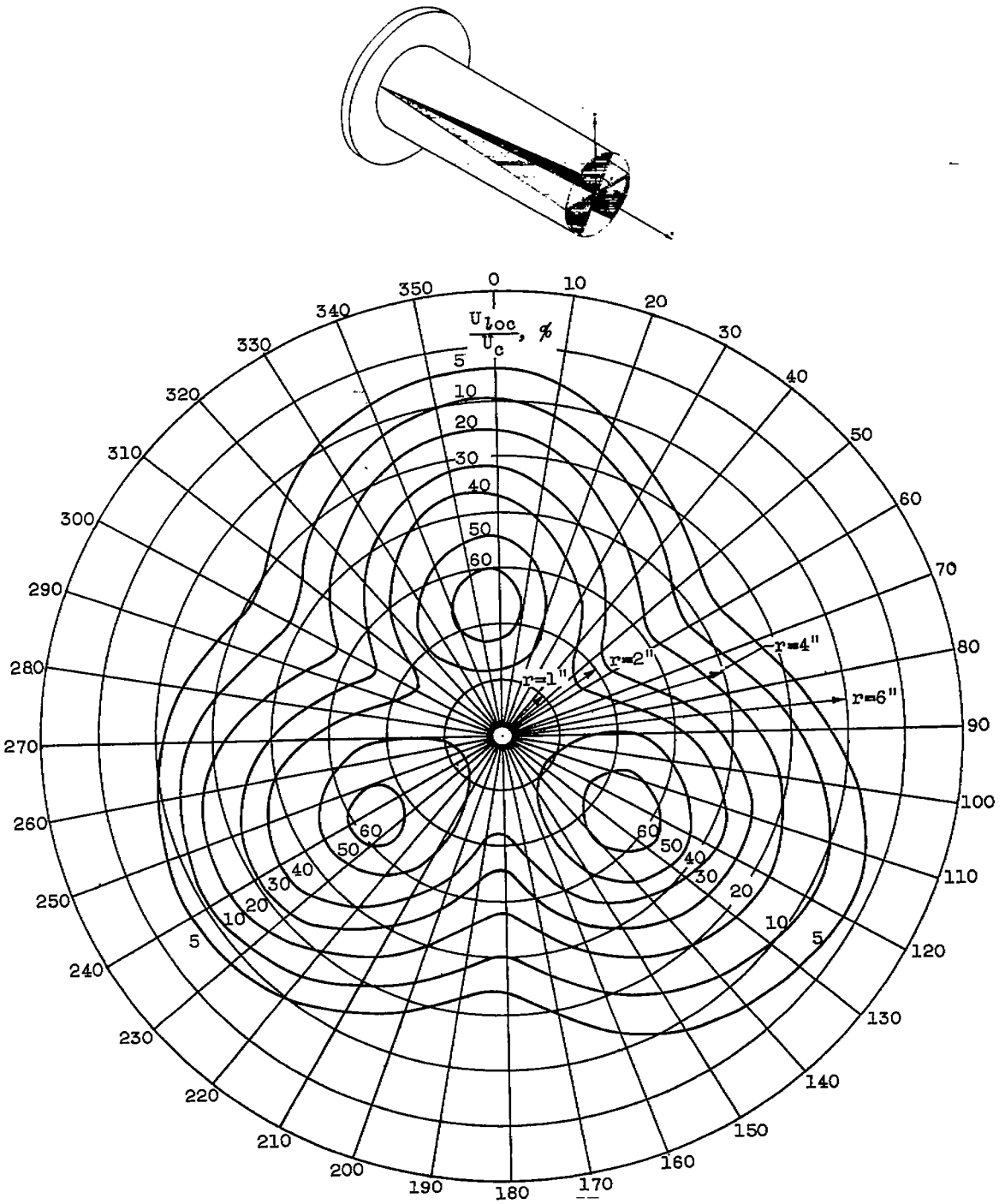

(e) Distance from nozzle, 24 inches.

Figure 4. - Concluded. Mean-flow maps for three-sector nozzle in x-θ plane. Mach number, 0.3; Reynolds number, 2.06×10^6 per foot.

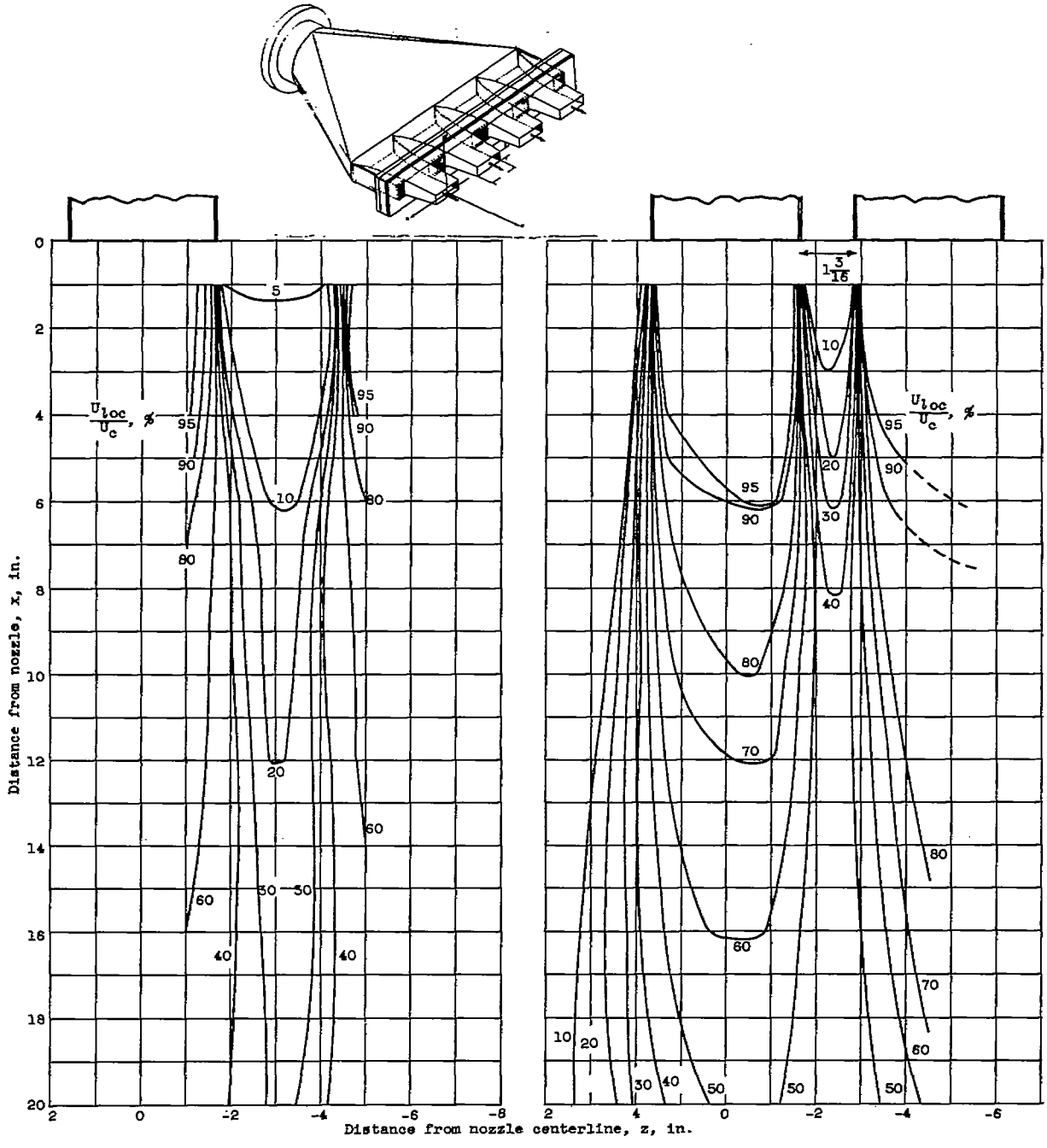

(a) Nozzle spacing, 2.95 inches. (b) Nozzle spacing, 1.19 inches.

Figure 5.- Mean-flow maps for rectangular slotted nozzle in x-z plane. Mach number, 0.3; Reynolds number, 2.06×10^6 per foot.

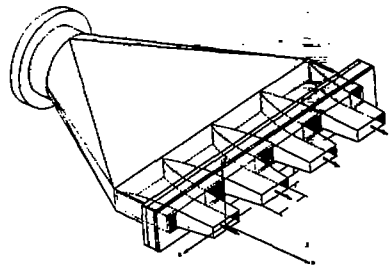

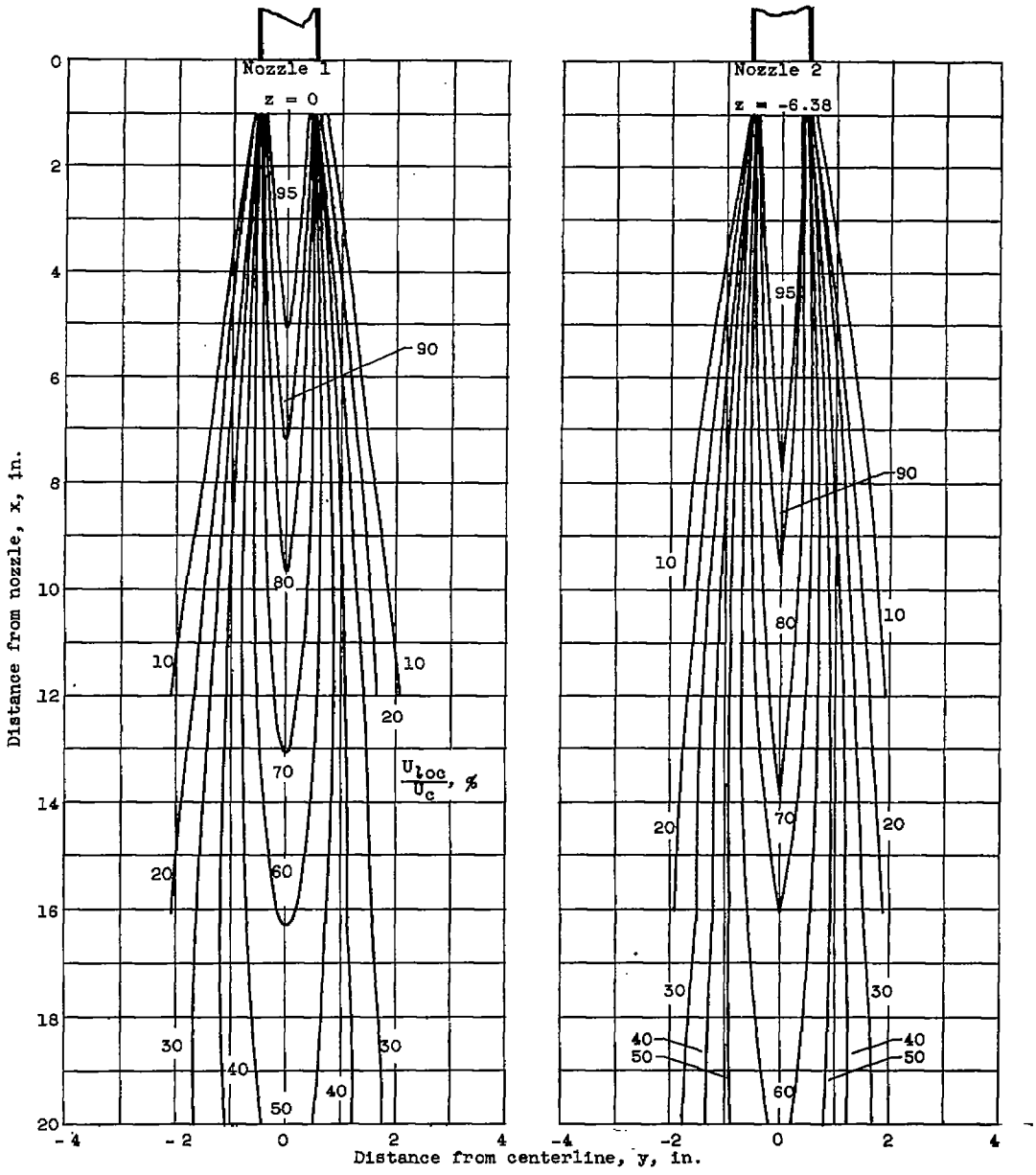

(a) Nozzle spacing, 2.95 inches.

Figure 6. - Mean-flow maps for rectangular slotted nozzle in x-y plane. Mach number, 0.3; Reynolds number, 2.06×10^6 per foot.

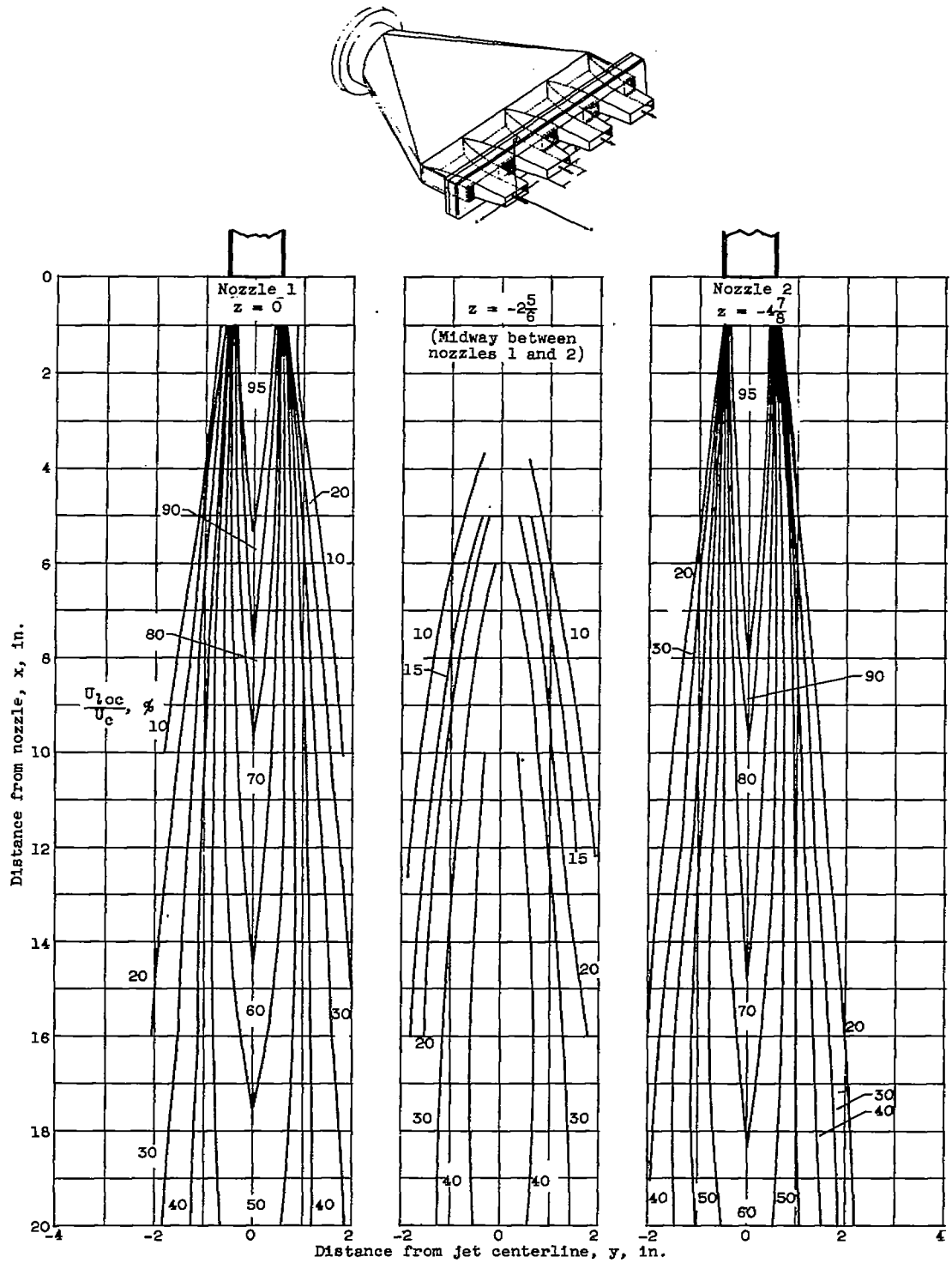

(b) Nozzle spacing, 1.19 inches.

Figure 6. - Concluded. Mean-flow maps for rectangular slotted nozzle in x-y plane. Mach number 0.3; Reynolds number, 2.06×10^6 per foot.

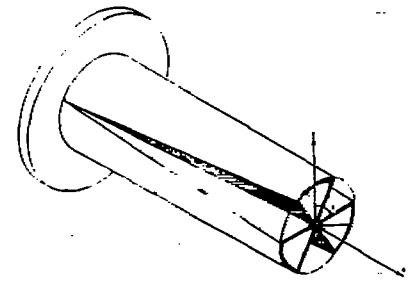

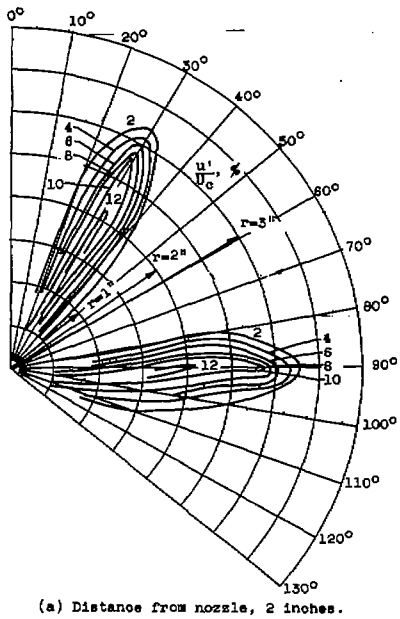

(a) Distance from nozzle, 2 inches.

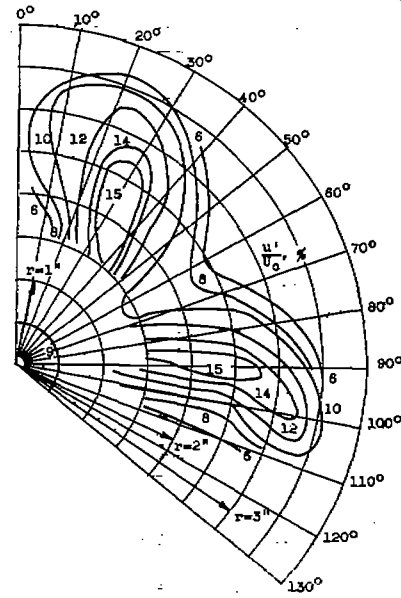

(c) Distance from nozzle, 8 inches.

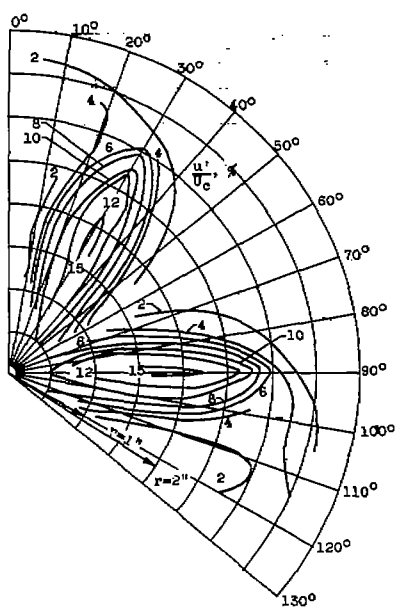

(b) Distance from nozzle, 4 inches.

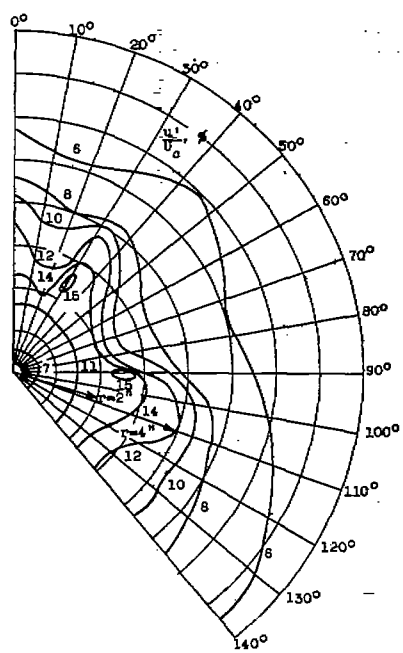

(d) Distance from nozzle, 12 inches.

Figure 7. - Intensity-of-turbulence maps for three-sector nozzle in r-θ plane. Mach number, 0.3; Reynolds number, 2.06×10^6 per foot; $\theta = 0°$ to 130°.

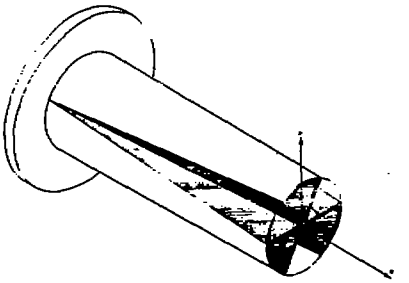

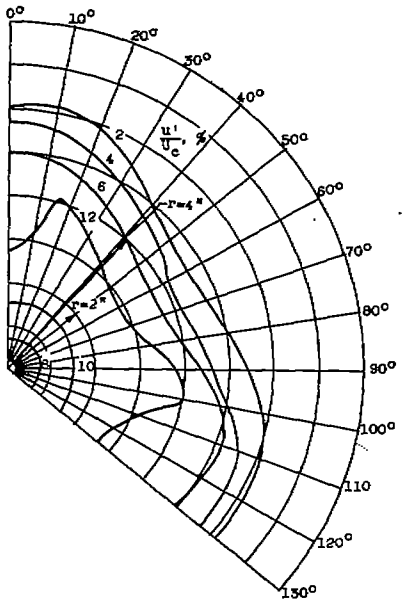

(e) Distance from nozzle, 16 inches.

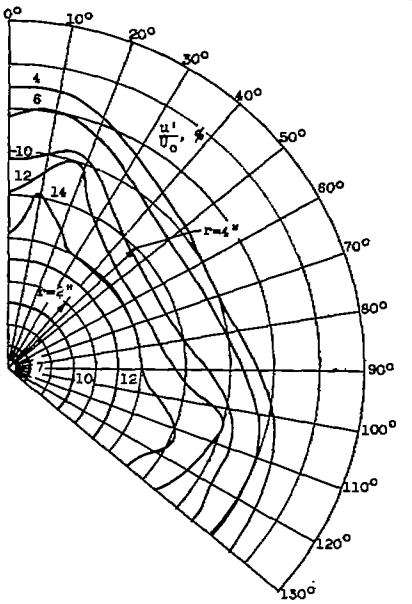

(g) Distance from nozzle, 24 inches.

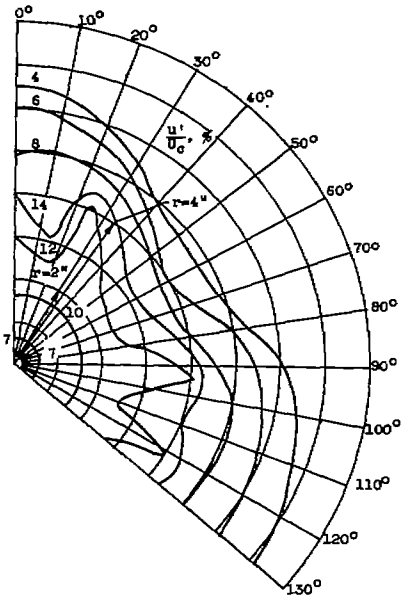

(f) Distance from nozzle, 20 inches.

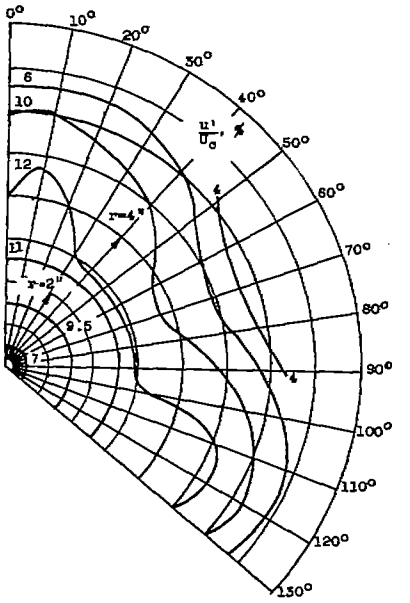

(h) Distance from nozzle, 28 inches.

Figure 7. - Concluded. Intensity-of-turbulence maps for three-sector nozzle in r-θ plane. Mach number, 0.3; Reynolds number, 2.06×10^6 per foot; $\theta = 0^0$ to 130^0.

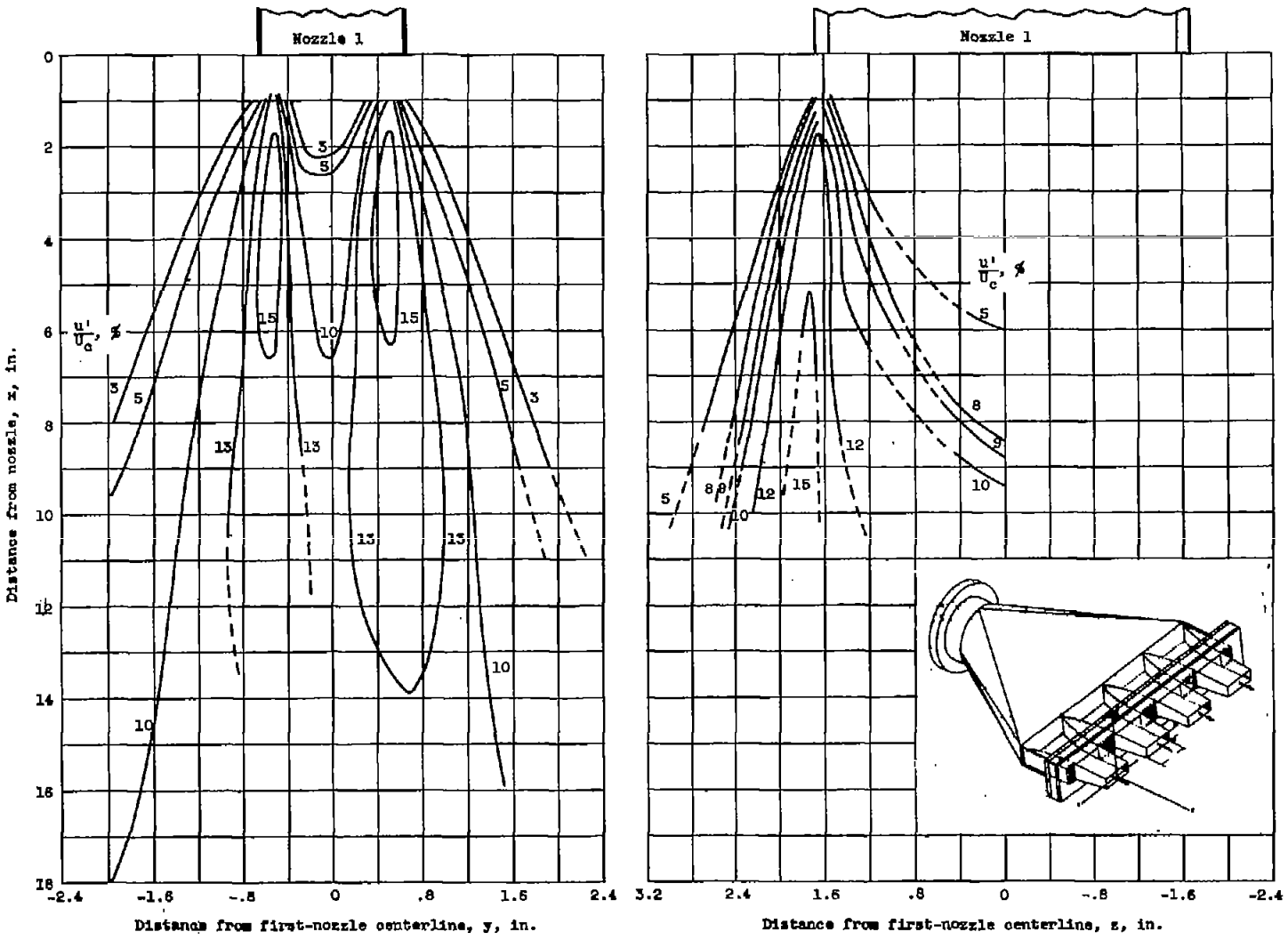

(a) Nozzle 1, x-y plane.

(b) Nozzles 1 and 2, x-z plane.

Figure 8. - Intensity-of-turbulence maps for rectangular slotted nozzle. Mach number, 0.3; Reynolds number, 2.06×10^6 per foot; nozzle spacing, 1.18 inches.

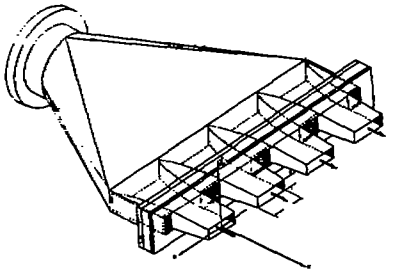

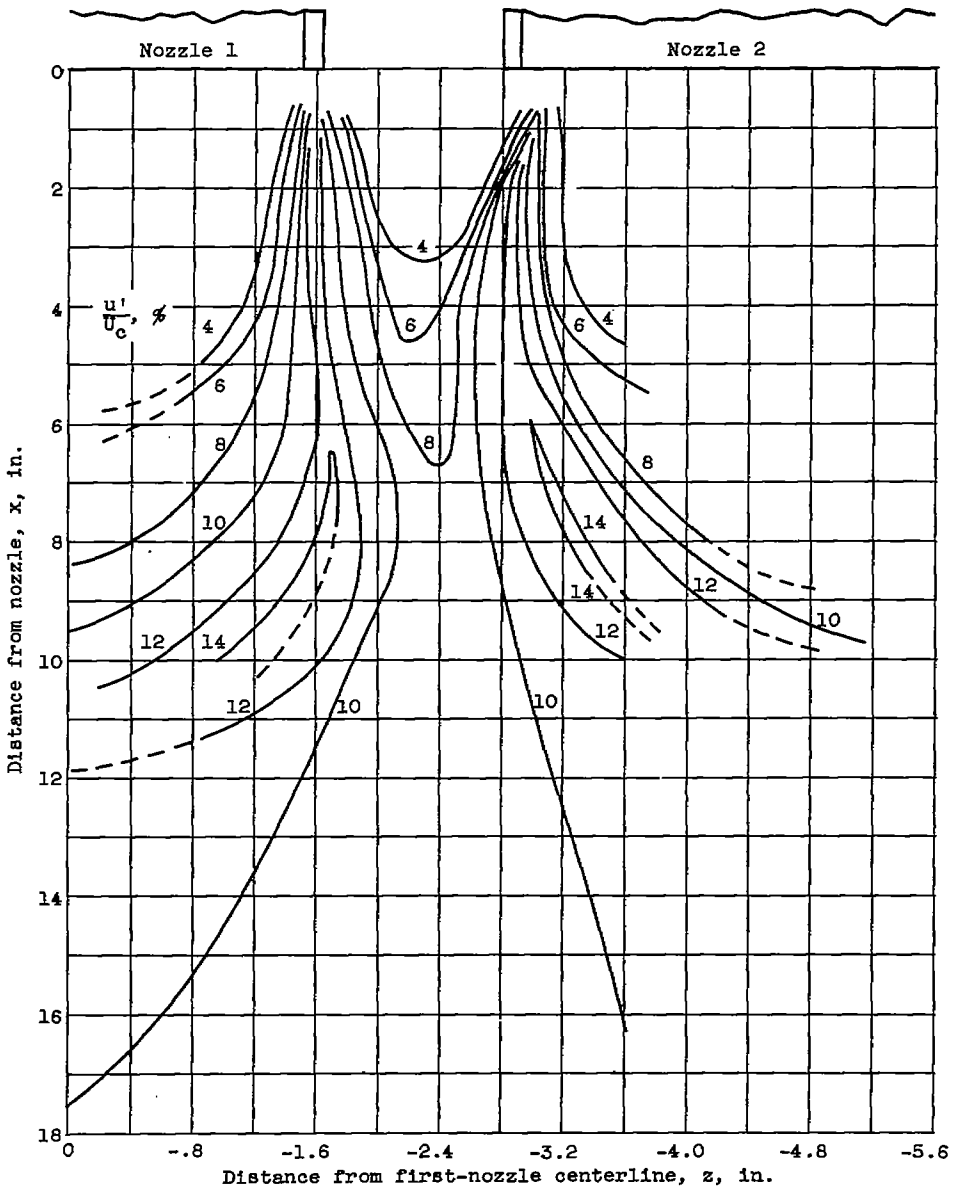

(c) Nozzles 1 and 2, x-z plane.

Figure 8. - Concluded. Intensity-of-turbulence maps for rectangular slotted nozzle. Mach number, 0.3; Reynolds number, 2.06×10^6 per foot; nozzle spacing, 1.19 inches.

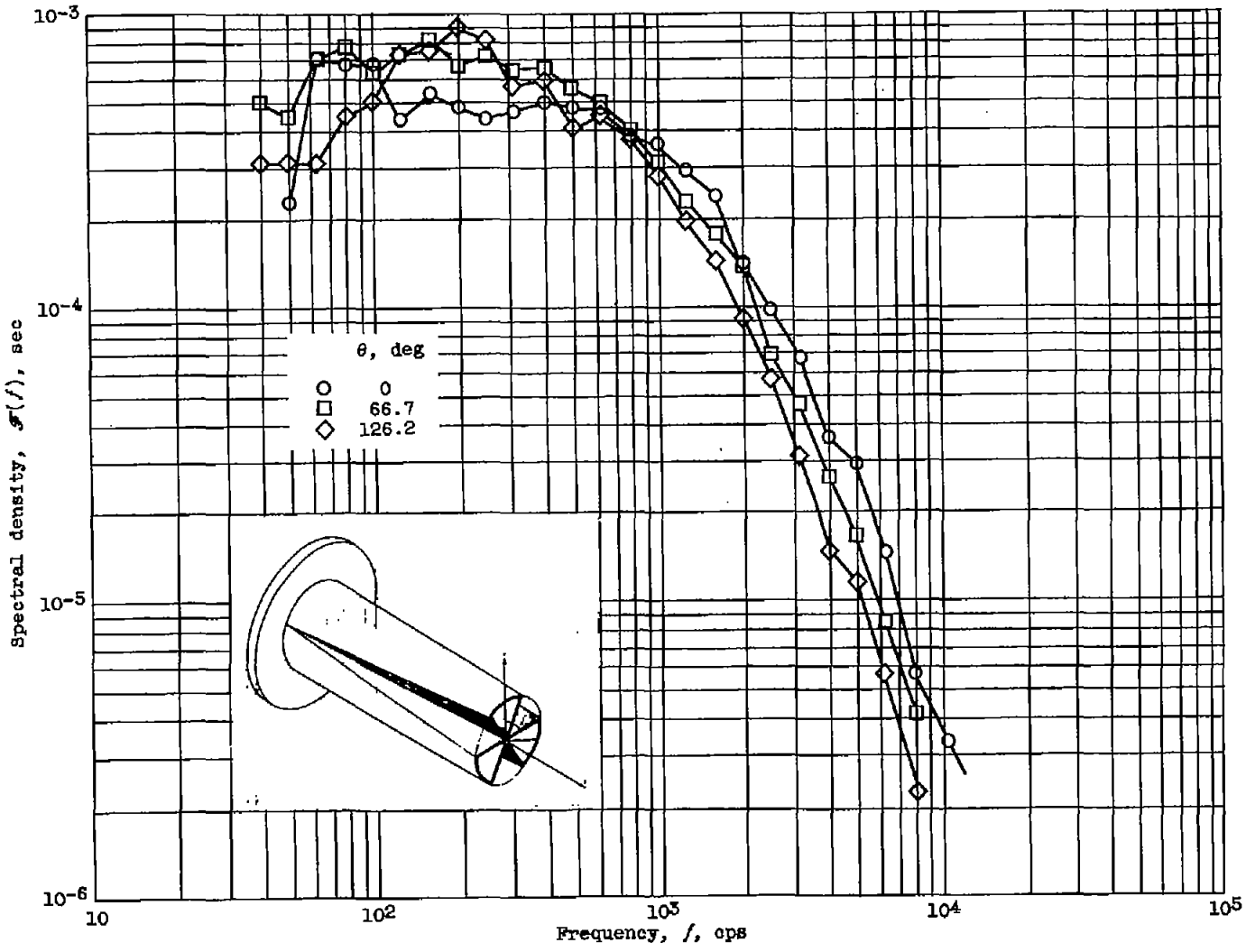

(a) Radial distance, 1/2 inch.

Figure 9. - Spectrum of turbulence for three-sector nozzle. Mach number, 0.3; Reynolds number, 2.06×10^6 per foot; distance from nozzle, 4 inches.

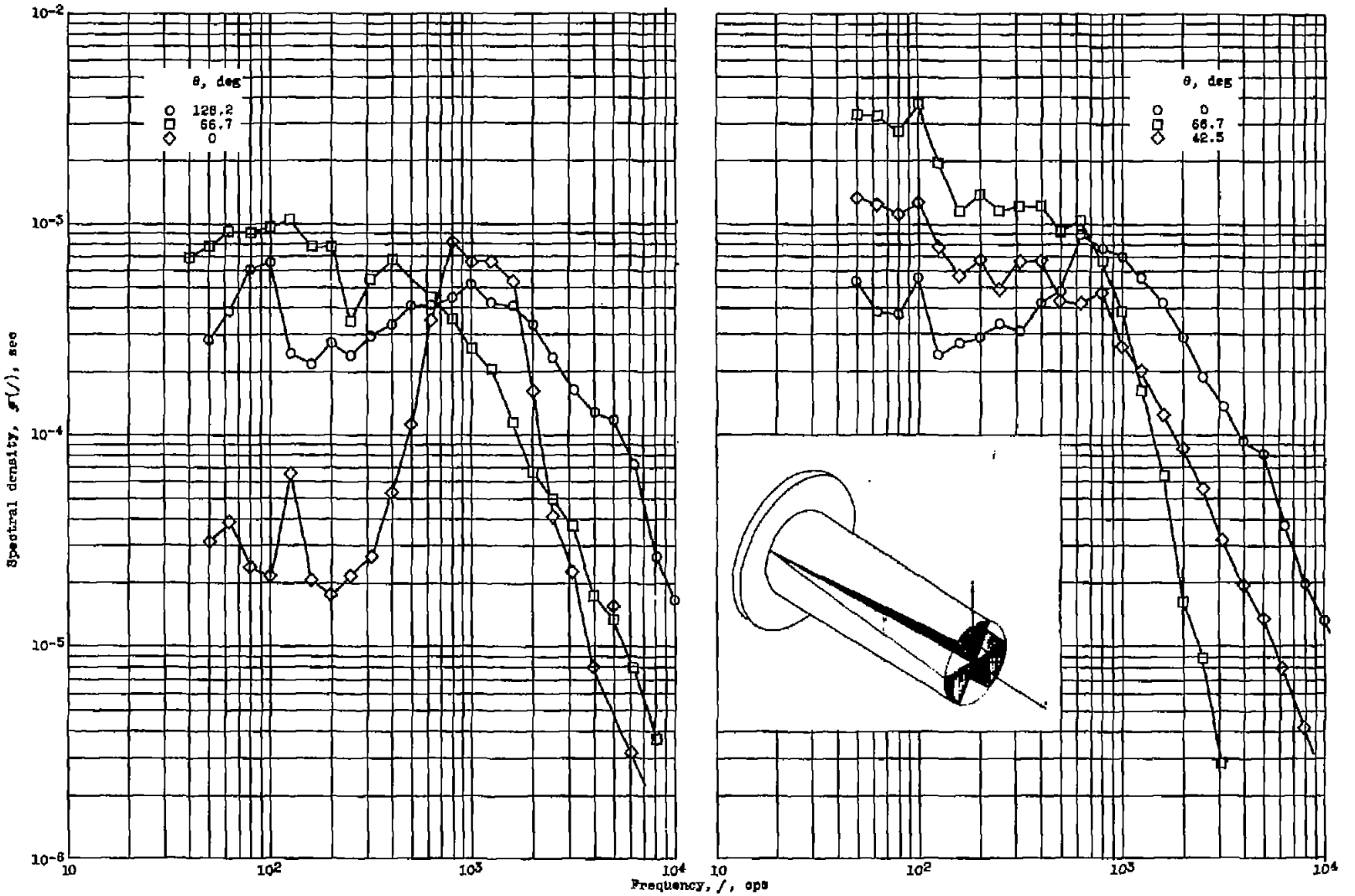

(b) Radial distance, $1\frac{1}{2}$ inches.

(c) Radial distance, $2\frac{1}{2}$ inches.

Figure 8. - Concluded. Spectrum of turbulence for three-sector nozzle. Mach number, 0.3; Reynolds number, 2.06×10^6 per foot; distance from nozzle, 4 inches.

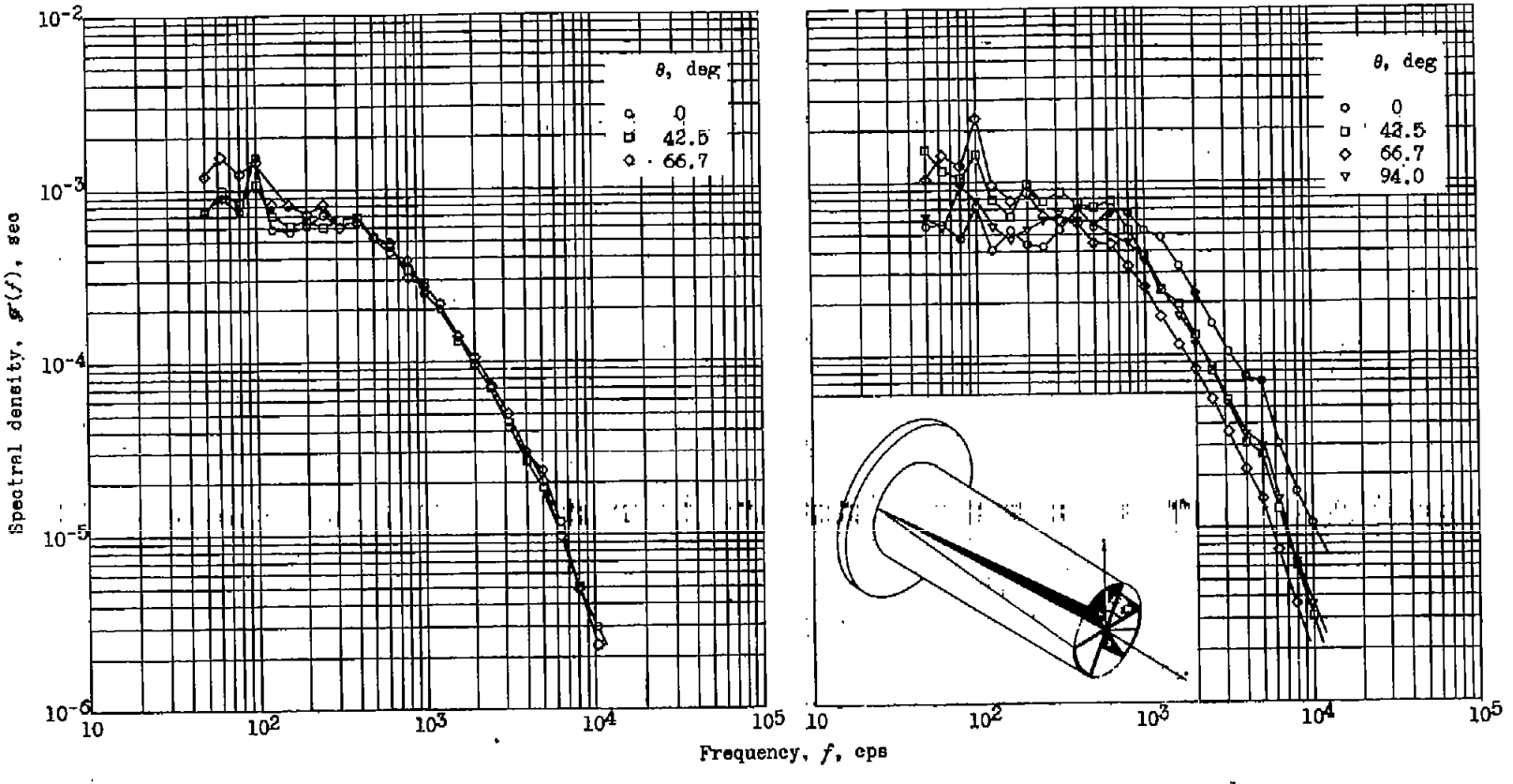

(a) Radial distance, 1/2 inch.

(b) Radial distance, $1\frac{1}{2}$ inches.

Figure 10. - Spectrum of turbulence for three-sector nozzle. Mach number, 0.3; Reynolds number, 2.06×10^6 per foot; distance from nozzle, 8 inches.

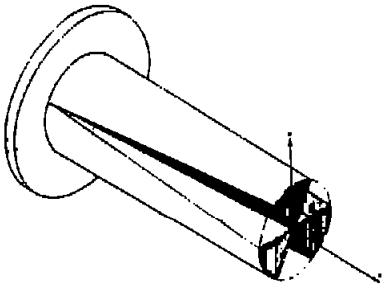

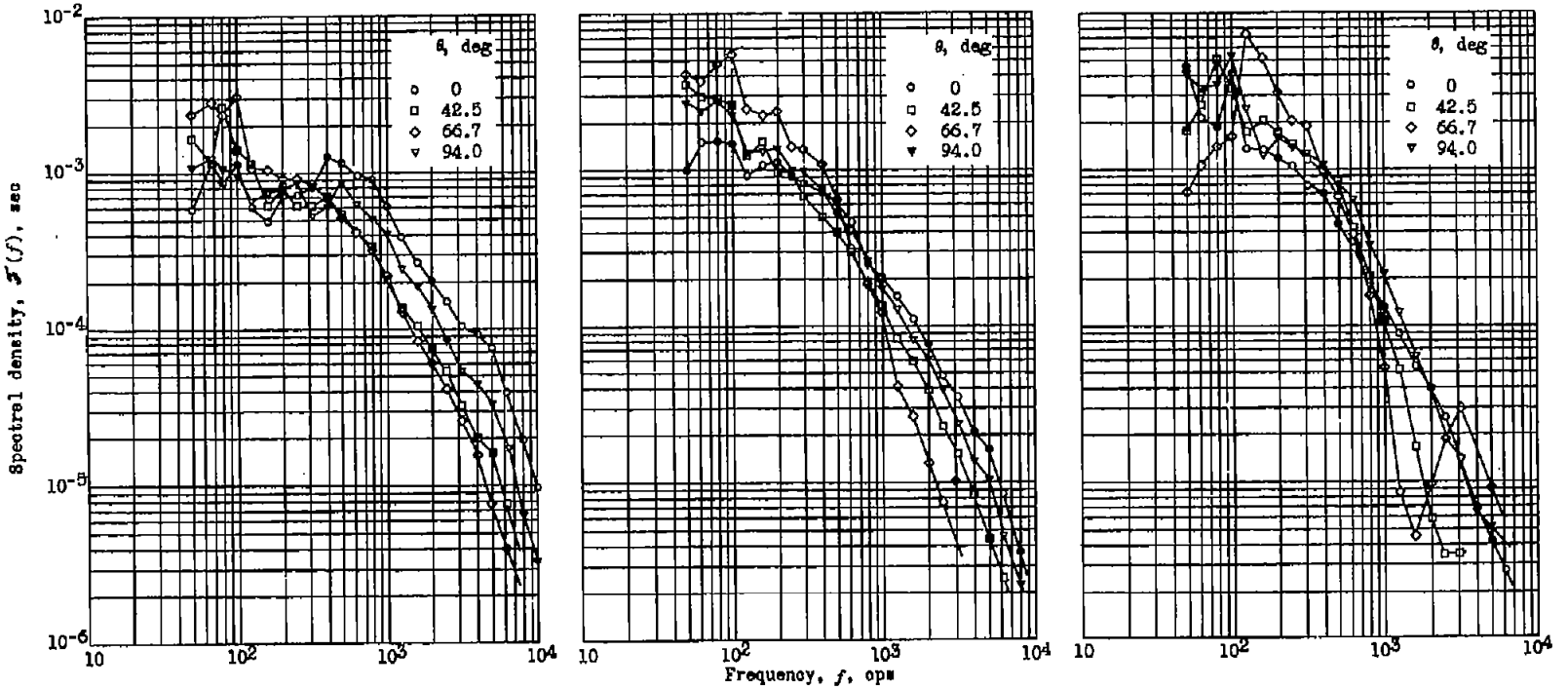

(c) Radial distance, $2\frac{1}{2}$ inches. (d) Radial distance, $3\frac{1}{2}$ inches. (e) Radial distance, 4 inches.

Figure 10. - Concluded. Spectrum of turbulence for three-sector nozzle. Mach number, 0.3; Reynolds number, 2.06×10^6 per foot; distance from nozzle, 8 inches.

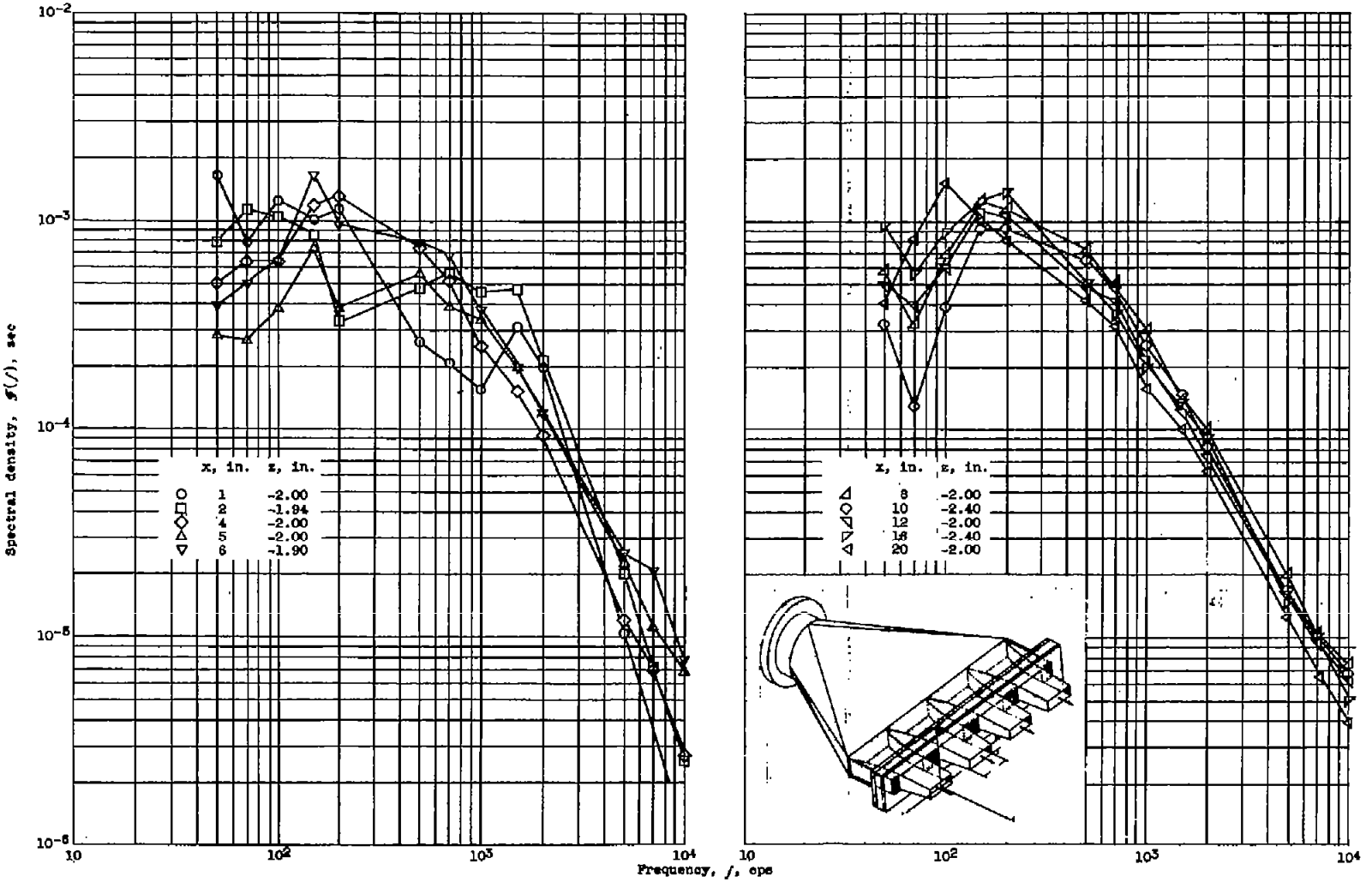

(a) Distances from the nozzle, 1, 2, 4, 5, and 6 inches.

(b) Distances from the nozzle, 8, 10, 12, 18, and 20 inches.

Figure 11. - Spectrum of turbulence for rectangular slotted nozzle. Mach number, 0.3; Reynolds number, 2.08×10^6 per foot; points in common mixing zone of nozzles 1 and 2; y = 0.

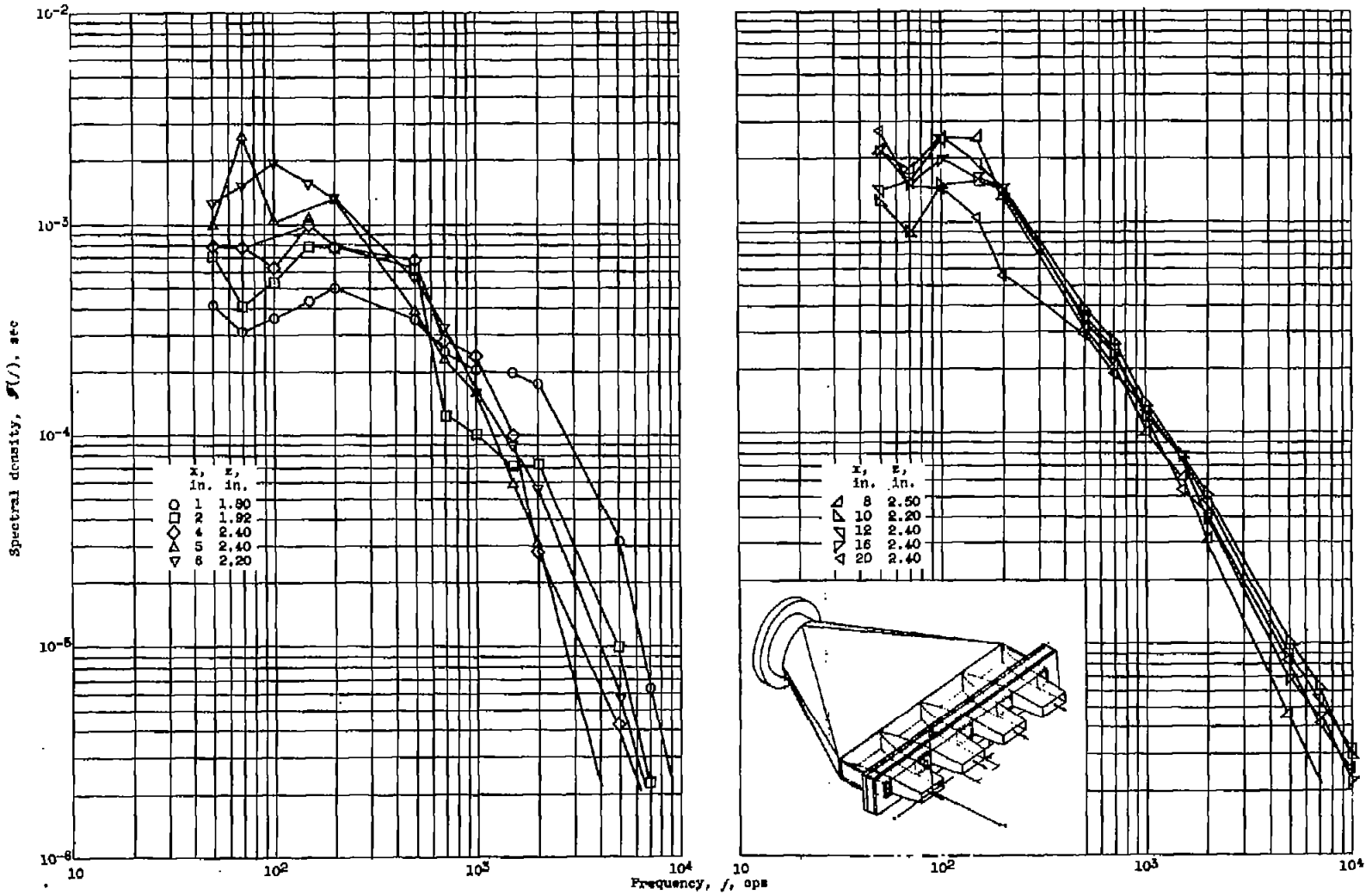

(a) Distances from the nozzle, 1, 2, 4, 5, and 6 inches.

(b) Distances from the nozzle, 8, 10, 12, 16, and 20 inches.

Figure 12. - Spectrum of turbulence for rectangular slotted nozzle. Mach number, 0.3; Reynolds number, 2.06×10^6 per foot; points in mixing zone of nozzle 1 alone; y = 0.

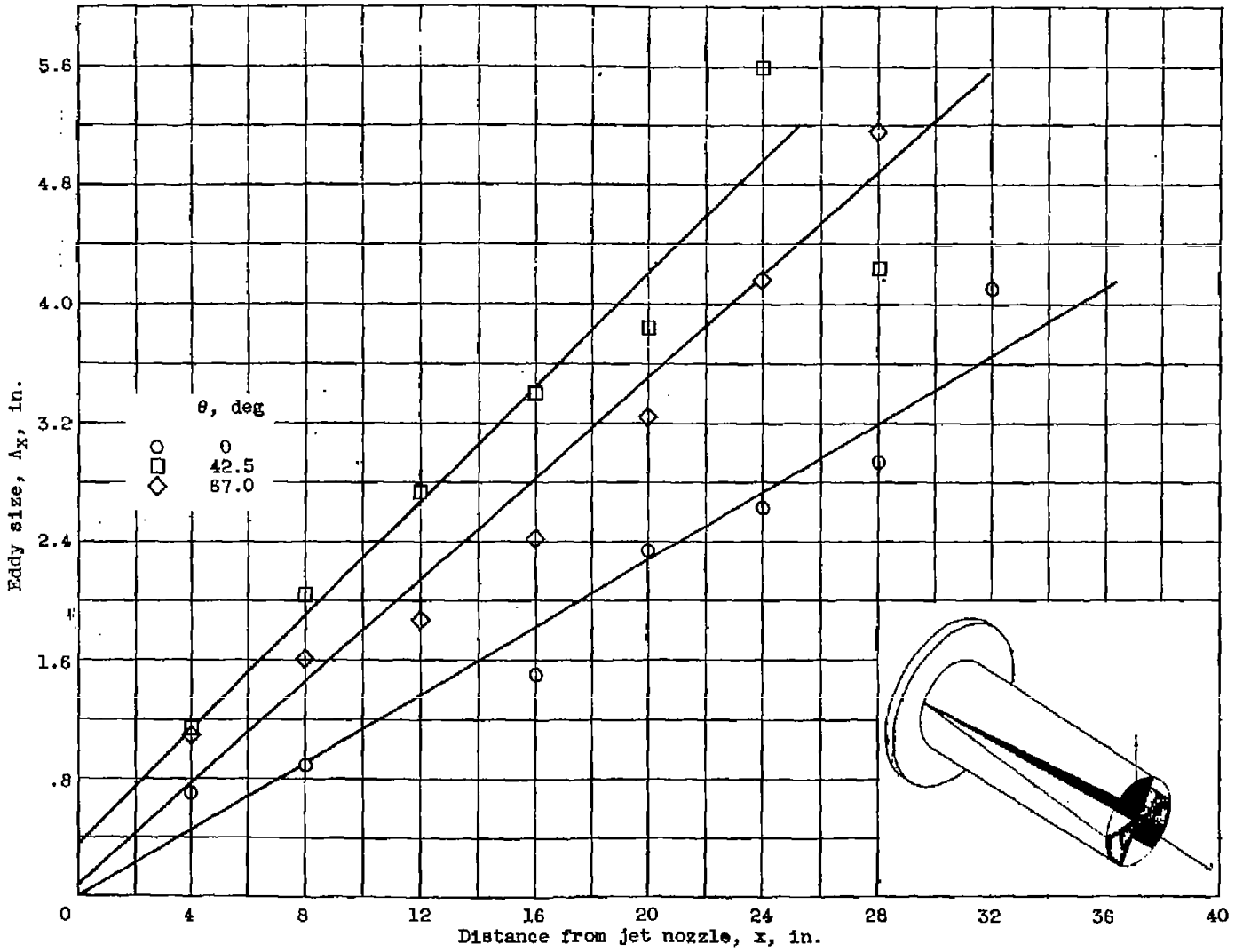

(a) Three-sector nozzle. Radial distance, $1\frac{1}{2}$ inches.

Figure 13. - Variation of eddy size with distance from jet nozzle. Mach number, 0.3; Reynolds number, 2.06×10^6 per foot.

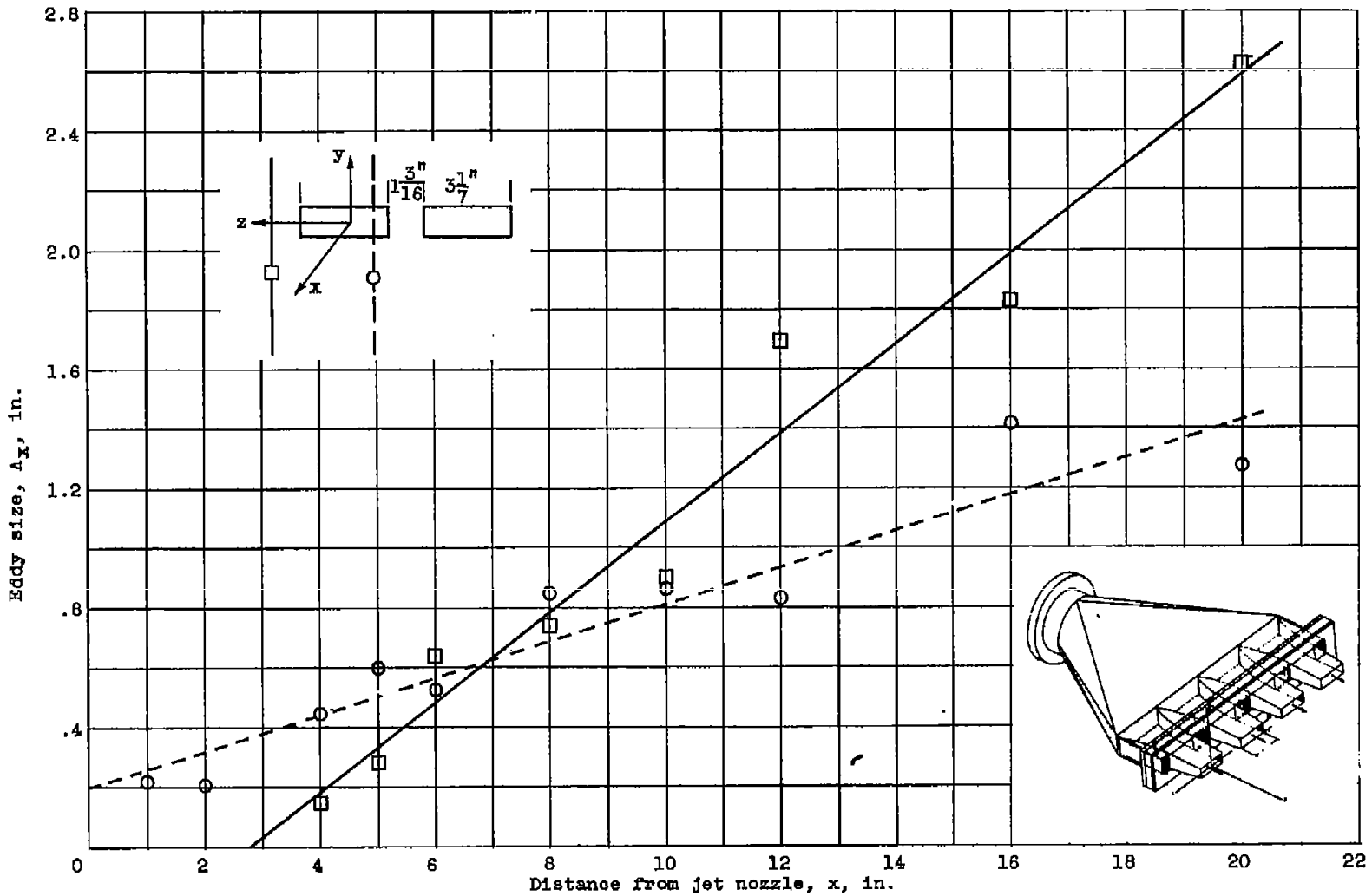

(b) Rectangular slotted nozzle.

Figure 13. - Concluded. Variation of eddy size with distance from jet nozzle. Mach number, 0.3; Reynolds number, 2.06×10^6 per foot.